




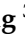
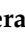




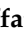




Review

# Space Photometry with BRITE-Constellation §

Werner W. Weiss <sup>1,\*</sup>, Konstanze Zwintz <sup>2</sup>, Rainer Kuschnig <sup>3</sup>, Gerald Handler <sup>4</sup>, Anthony F. J. Moffat <sup>5</sup>,  
Dietrich Baade <sup>6</sup>, Dominic M. Bowman <sup>7</sup>, Thomas Granzer <sup>8</sup>, Thomas Kallinger <sup>1</sup>, Otto F. Koudelka <sup>3</sup>,  
Catherine C. Lovekin <sup>9</sup>, Coralie Neiner <sup>10</sup>, Herbert Pablo <sup>11</sup>, Andrzej Pigulski <sup>12</sup>, Adam Popowicz <sup>13</sup>,  
Tahina Ramiamanantsoa <sup>14</sup>, Slavek M. Rucinski <sup>15</sup>, Klaus G. Strassmeier <sup>8</sup> and Gregg A. Wade <sup>16</sup>

- <sup>1</sup> Institute for Astrophysics, University of Vienna, A-1180 Vienna, Austria; kallinger@astro.univie.ac.at
  - <sup>2</sup> Institute for Astro- and Particle Physics, University of Innsbruck, A-6020 Innsbruck, Austria; konstanze.zwintz@uibk.ac.at
  - <sup>3</sup> Institut für Kommunikationsnetze und Satellitenkommunikation, Technische Universität Graz, A-8020 Graz, Austria; rainer.kuschnig@tugraz.at (R.K.); koudelka@TUGraz.at (O.F.K.)
  - <sup>4</sup> Nicolaus Copernicus Astronomical Center, Polish Academy of Sciences, 00-716 Warsaw, Poland; gerald@camk.edu.pl
  - <sup>5</sup> Department of Physics, University of Montreal, Montreal, QC H3C 3J7, Canada; amoffat@sympatico.ca
  - <sup>6</sup> European Southern Observatory (ESO), D-85748 Garching bei München, Germany; dbaade@eso.org
  - <sup>7</sup> Institute of Astronomy, KU Leuven, B-3001 Leuven, Belgium; dominic.bowman@kuleuven.be
  - <sup>8</sup> Department Cosmic Magnetic Fields, Leibniz Institut fuer Astrophysik Potsdam, D-14482 Potsdam, Germany; tgranzer@aip.de (T.G.); kstrassmeier@aip.de (K.G.S.)
  - <sup>9</sup> Physics Department, Mount Allison University, Sackville, NB E4L 1E6, Canada; clovekin@mta.ca
  - <sup>10</sup> LESIA, Paris Observatory, PSL University, CNRS, Sorbonne Université, Université de Paris, 92195 Meudon, France; coralie.neiner@obspm.fr
  - <sup>11</sup> American Association of Variable Star Observers (AAVSO), Cambridge, MA 02138, USA; hpablo@aaavso.org
  - <sup>12</sup> Instytut Astronomiczny, Uniwersytet Wrocławski, 51-622 Wrocław, Poland; pigulski@astro.uni.wroc.pl
  - <sup>13</sup> Department of Electronics, Electrical Engineering and Microelectronics, Silesian University of Technology, 44-100 Gliwice, Poland; Adam.Popowicz@polsl.pl
  - <sup>14</sup> School of Earth and Space Exploration, Arizona State University, Tempe, AZ 85287, USA; tahina@asu.edu
  - <sup>15</sup> Department of Astronomy and Astrophysics, University of Toronto, Toronto, ON M5S 3H4, Canada; rucinski@astro.utoronto.ca
  - <sup>16</sup> Department of Physics and Space Science, Royal Military College of Canada, Kingston, ON K7k7b4, Canada; Gregg.Wade@rmc.ca
- \* Correspondence: werner.weiss@univie.ac.at
- § BRITE-Constellation was designed, built, launched, and is operated and supported by the Austrian Research Promotion Agency (FFG), the University of Vienna, the Technical University of Graz, the University of Innsbruck, the Canadian Space Agency (CSA), the University of Toronto Institute for Aerospace Studies (UTIAS), the Foundation for Polish Science & Technology (FNiTP MNiSW) and the National Science Centre (NCN).



**Citation:** Weiss, W.W.; Zwintz, K.; Kuschnig, R.; Handler, G.; Moffat, A.F.J.; Baade, D.; Bowman, D.M.; Granzer, T.; Kallinger, T.; Lovekin, C.C.; et al. Space Photometry with BRITE-Constellation. *Universe* **2021**, *7*, 199. <https://doi.org/10.3390/universe7060199>

Academic Editors: Laszlo Szabados and Nikolay N. Samus

Received: 17 May 2021  
Accepted: 8 June 2021  
Published: 16 June 2021

**Publisher's Note:** MDPI stays neutral with regard to jurisdictional claims in published maps and institutional affiliations.



**Copyright:** © 2021 by the authors. Licensee MDPI, Basel, Switzerland. This article is an open access article distributed under the terms and conditions of the Creative Commons Attribution (CC BY) license (<https://creativecommons.org/licenses/by/4.0/>).

**Abstract:** BRITE-Constellation is devoted to high-precision optical photometric monitoring of bright stars, distributed all over the Milky Way, in red and/or blue passbands. Photometry from space avoids the turbulent and absorbing terrestrial atmosphere and allows for very long and continuous observing runs with high time resolution and thus provides the data necessary for understanding various processes inside stars (e.g., asteroseismology) and in their immediate environment. While the first astronomical observations from space focused on the spectral regions not accessible from the ground it soon became obvious around 1970 that avoiding the turbulent terrestrial atmosphere significantly improved the accuracy of photometry and satellites explicitly dedicated to high-quality photometry were launched. A perfect example is BRITE-Constellation, which is the result of a very successful cooperation between Austria, Canada and Poland. Research highlights for targets distributed nearly over the entire HRD are presented, but focus primarily on massive and hot stars.

**Keywords:** space photometry; stellar structure; stellar evolution; stellar environment; nanosatellites

## 1. A Brief Flashback

The first successful launch of a satellite in 1957 (Sputnik [1]) triggered a new era of astronomical observing techniques which enormously expanded the research potential of astrophysics, mainly because the terrestrial atmosphere could be overcome. Consequently, the first space observations focused on spectral regions, which were not accessible from the ground. Eight years after Sputnik, Proton satellites observed cosmic  $\gamma$ -rays (1965). The Orbiting Astronomical Observatory (OAO [2]) from NASA were the first operational telescopes in space. After a power failure of OAO-1 right after the launch in 1966, OAO-2 was launched in 1968, and a follow-up, OAO-3 (Copernicus), was launched in 1972. These OAO-satellites provided a wealth of insight into the variability of stars and intricate details of the interstellar matter. The Astronomical Netherlands Satellite (ANS, 1974 [3]) conducted photometric observations of variable stars in the UV, followed by the NASA/ESA International Ultraviolet Explorer (IUE [4]) in 1978.

Already in the early days of space astronomy, the obvious scientific success accelerated the development of space instrumentation for all spectral ranges, taking advantage of avoiding a turbulent and absorbing atmosphere, not to mention clouds and a day/night rhythm. The desire to observe even fainter targets required the launch of space telescopes with increasing size—very similar to most ground based observatories. A still scientifically productive example is the amazing Hubble Space Telescope (HST [5]), launched in 1990.

It needed nearly 30 years after the dawn of space telescopes for projects explicitly dedicated to “simple” stars to become a reality. A most prominent example is Hipparcos [6], an ESA mission with an aperture of 29 cm, launched in 1989, with the goal of determining high precision parallaxes of a large number of stars in our neighbourhood. The entire sky was scanned during three years, which resulted in up to 110 data points per star in the final Hipparcos and Tycho catalogues. The data have proven to be a treasure chest for detecting stellar variability (Kallinger and Weiss [7] and many more). The follow-up ESA mission Gaia ([8]), using a  $145 \times 50$  cm telescope, was launched in 2013 and enormously increased our knowledge about the 4D picture of our Galaxy.

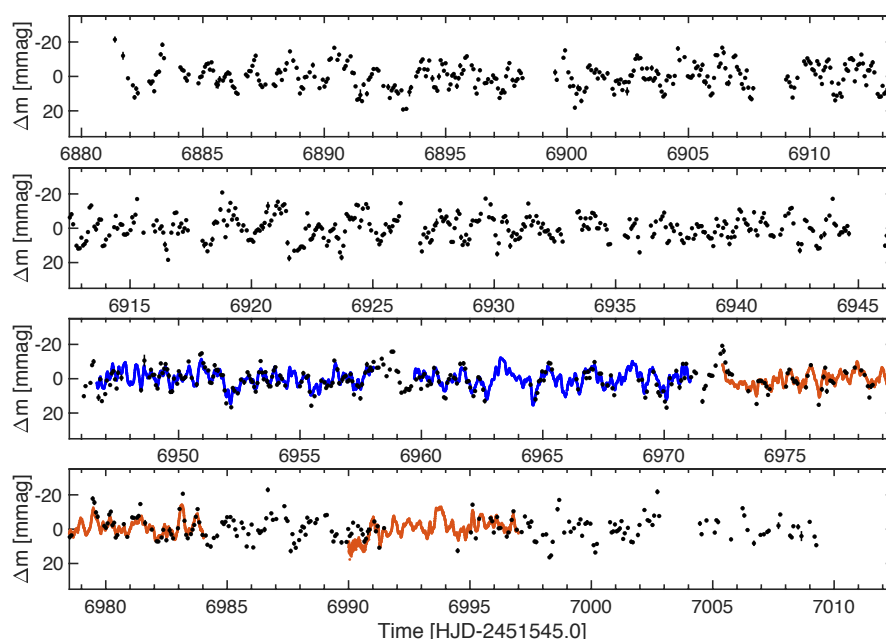
Projects in the early stages of space telescopes focused on highly ranked targets devoted to the evolutionary aspects of galaxies, cosmology, interstellar nebulae and their role in stellar evolution, solar system planets and other hot topics. Monitoring classical variable or allegedly constant stars continuously over many hours, days or even months, was hindered due to the high pressure on telescope time. Fortunately, space telescopes need pointing and guiding equipment, usually provided by small auxiliary telescopes. One of the first star trackers, “abused” for stellar photometry, was the Fine Guidance Sensor (FGS) of the HST, as described by [9–13] and in workshop proceedings of the Space Telescope Science Institute (Kuschnig et al. [14]).

Already in 1982, a first proposal for a space photometer dedicated to stellar variability and activity, Evris, was submitted to CNES (Mangeney et al. [15]) and was developed further as a passenger instrument for the USSR-Mars94 mission. It was intended to be active during the cruise time to Mars (Vuillemin et al. [16]). However, launch of the Mars94 mission was delayed to 1996 and ended in disaster, because of a rocket failure, which crashed Mars96 in the Chilean Andes together with Evris. Fortunately, the experience gained during development of Evris was not lost: already in 1993, the French team had submitted a larger follow-up seismology mission, CoRoT (Schneider et al. [17], Weiss and Baglin [18]), which was launched by ESA in 2006 and was active until 2014.

Asteroseismology experienced a boom towards the end of the last century, as it became obvious how much one can learn about stellar structure and evolution with this tool, as well as how one can test complex astrophysical concepts, with important implications for astrophysics in general. However, excellent data were necessary for such investigations, that is, data which cover as continuously as possible a long time span and with mmag accuracy or better.

A textbook-like example is  $\zeta$  Pup (Figure 1), which was observed simultaneously from space by two satellites and which illustrates the bonus of higher photometric accuracy

(TESS) counter-weighted by longer data sets (BRITe). Another example is  $\alpha$  Cir (Section 4.12 and Figure 20). The shorter TESS run of  $\zeta$  Pup has broader Fourier peaks ( $\approx 1.5$  months vs.  $\approx 4.5$  months long data sets), but also shows many Fourier peaks, which appear to be less prominent in a longer run as is illustrated in the time resolved frequency analysis (lower part of Figure 2). Evidently, stochastic stellar variability dominates in the shorter run, while the 1.78 d cyclic variability of the star is much more well-defined and well-covered in the longer observing run (see also Figure 1). The changing amplitude of the 1.78 d signal indicates that the signal is likely due to (bright) spots of this O4If(n) type star that come and go. Sometimes the signal is not even there (see the BHR time-frequency diagram of Figure 2). Whenever there are overlapping TESS and BHR observations, they follow each other relatively well and have roughly the same amplitudes, except at the beginning of each subset of the TESS observations, which is due to systematics in TESS data around gaps. More about  $\zeta$  Pup is presented later in Section 4.1, including comments on the physics that is probably involved.

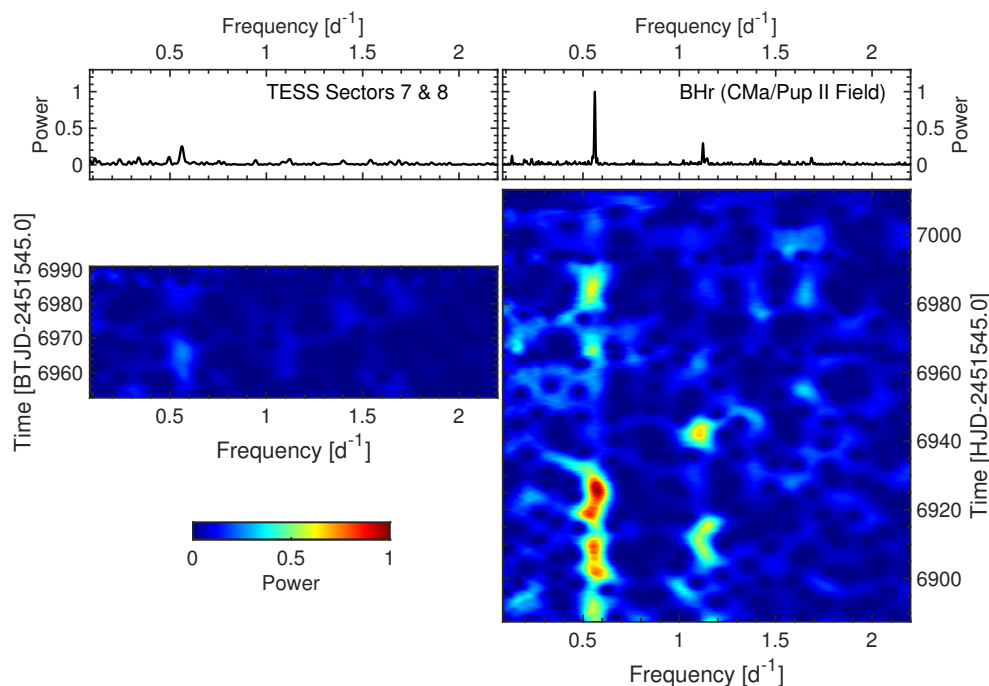


**Figure 1.**  $\zeta$  Pup observed by BRITe-Heweliusz, a component of BRITe-Constellation, (black dots, red filter) and with TESS in sector 7 (first line in blue) and in sector 8 (second line in red).

In addition to long continuous data sets, photometers operated in space have an advantage by avoiding day-time gaps in low-Earth orbits, inaccessibility of stars during certain seasons, and noise introduced by a turbulent atmosphere (Weiss [19]). The need for such data was subsequently boosted further by the discovery of exoplanets.

The CNES mission CoRoT provides a perfect example of a “small” satellite, which produced top science with a rather small budget, although nowhere nearly as small as that for BRITe-Constellation. Not surprisingly, the scientific community was interested in generating more such satellites, but competition with trendy space projects was intense, as is illustrated by the tortuous path after CoRoT. PRISMA (Lemaire et al. [20]) was developed to extend CoRoT and was accepted in 1993 as an ESA Horizon-2000 M2 project study, but finally lost the race in 2002 against the  $\gamma$ -ray satellite INTEGRAL. The study team did not give up and produced a Horizon-2000 M3 proposal, STARS (Jones et al. [21]), but lost again in 2009 against the cosmic background explorer Planck. The next attempt was Eddington (Favata et al. [22], Roxburgh [23]), an ESA Flexi Mission, but the gravitational wave detector Lisa settled its problems for a planned launch in 2015, and consequently Eddington had to step back. Later, the launch of LISA was delayed and is now scheduled for 2034. But finally, PLATO was proposed in 2007 and selected in 2014 as an ESA Cosmic Vision mission (PLATO-Consortium [24]), driven by an exploding interest in exoplanets.

Launch is scheduled for 2026. It took 20 years after CoRoT till a follow-up, Plato, finally was decided and about 30 years till-hopefully-first data will be available!



**Figure 2.** Time dependent frequency spectra of  $\zeta$  Pup obtained from data presented in Figure 1 (Ramiamanantsoa et al., in preparation) and with a sliding time window of 12 days. The colour scale represents signal power normalized to the maximum power in the windowed discrete Fourier transforms of the BHR data.

Outside Europe, similar efforts were also successful. Soon after the crash of Evris, an Announcement of Opportunity (AO) for Small Payloads was distributed in 1996 by the Canadian Space Agency (CSA), which was responded to in 1997 with a proposal for MOST (Rucinski et al. [25]). This satellite was launched in 2003 as Canada's first space telescope, and with an aperture of 15 cm it was the smallest space telescope in orbit at that time. While designed only for a nominal lifetime of one year, it collected under the directorship of Jaymie Matthews (UBC) scientifically useful data till January 2018, that is, for more than 15 years. Even after the CSA operations, funding ended in 2014, MOST was frequently activated for pay-per-view observers.

Paying tribute to the exploding interest in exoplanets after the detection of 51b Peg, NASA decided in 2001 to fund a space telescope, Kepler, dedicated to the discovery of exoplanets (Borucki et al. [26]). At that time only 80 exoplanets were known, a number which increased dramatically after Kepler's launch in 2009. Reaction-wheel failures in 2012 and 2013 resulted in a modified mission, Kepler-K2, which finally ended the mission in 2018, after the discovery of more than 2600 exoplanets and delivering an enormous amount of data for asteroseismology.

The Wide Field Infrared Explorer (WIRE) reminds one of the HST's Fine Guidance Sensors as auxiliary equipment with a potential for space photometry. WIRE (Hacking et al. [27]) was launched in 1999, but due to a premature ejection of the telescope cover, all cryogen quickly evaporated and made IR observation impossible. Fortunately, the star tracker was still working and contributed successfully to asteroseismology until the decommissioning of WIRE in 2011. This substantially exceeded the four months of the originally planned lifetime of the IR mission. Another mission producing photometric data for asteroseismology as a side-product to its main research goal is the Solar Mass Ejection Imager (SMEI) on board Coriolis (Eyles et al. [28]), which was operational from 2003 to 2011 in a sun synchronous polar orbit with 102 min period.

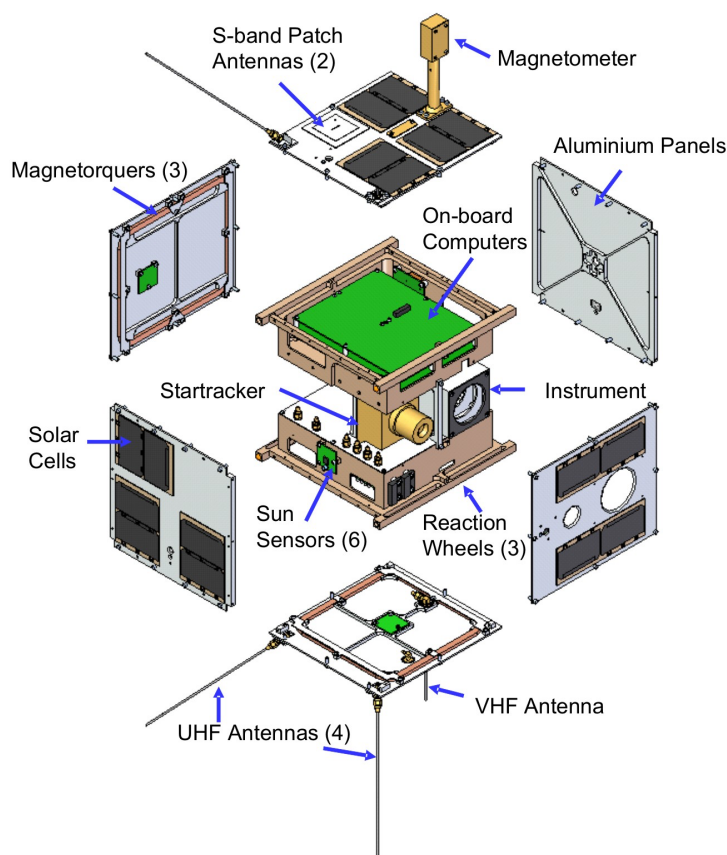


The follow-up mission to Kepler is TESS, which was first discussed in 2005 and launched in 2018 by NASA, just after ending the Kepler mission. TESS (Ricker et al. [29]) focuses on the stars brighter than those observed by Kepler and the K2 follow-up, and it covers a sky area 400 times larger than that monitored by Kepler. As an example of the relevance of TESS data for asteroseismology we refer, for example, to Cunha et al. [30], Antoci et al. [31], Bowman [32] and Burssens et al. [33].

More information about HST, Kepler, Gaia and TESS will be presented in dedicated chapters of this journal volume.

## 2. The Birth of BRITE-Constellation

The development of BRITE-Constellation can be traced to the origins of the Canadian microsatellite MOST [25], which was designed by Slavek Rucinski and Kieran Carroll (University of Toronto, UT), starting with construction in 1998, and successfully utilized by the team led by Jaymie Matthews (UBC) after launch in 2003 till 2014. Robert Zee (Manager of UT Space Flight Laboratory, SFL) wanted to continue the momentum created by the success of MOST and asked Rucinski in 2002 the non-trivial question, if nanosatellites could be of relevance for astronomy. One has to keep in mind that at that time nanosatellites were young and rarely utilized for research, with primary interest as an engineering experimentation exercise and looking down, not up, for Earth-atmosphere and -surface research. Nevertheless, a design concept for a single CANX-3 satellite was developed in 2004 by SFL and a small team of Canadian astronomers as a first fully three-axis stabilized satellite of  $20 \times 20 \times 20$  cm size, containing a telescope with 3 cm aperture (Figure 3).



**Figure 3.** Basic structure of the BRITE satellites. Source: SFL.

Another root of origin is with Werner Weiss (University of Vienna, UoV) who was co-I of Evris, later of CoRoT and also a member of the MOST team. The latter membership closed the loop to CanX-3. The failure of the Evris-launch contrasted dramatically with the

anticipated research potential for asteroseismology, an expectation, which was later confirmed by CoRoT and MOST. Hence, the pressure to produce a space telescope optimised for bright stars grew. Luckily, the Austrian Ministry of Science and Technology established in March 2005 a program for improving the infrastructure of Austrian Universities, to which UoV submitted a proposal for UNIBRITE. This was accepted in October 2005 and, one month later, UNIBRITE was ordered at SFL, based on their concept of CanX-3.

A third root is with Otto Koudelka (Technical University Graz, TUG). The Austrian Space Agency (ASA) issued in 2005 a call for the 3rd Austrian Space Programme. Two nanosatellite proposals were in the queue: one of the Institute for Astrophysics (UoV), dedicated to asteroseismology (Weiss [19]), and another from the Institute of Communication Networks and Satellite Communications (TUG), for developing and building a cubesat. ASA suggested to merge these initiatives, which resulted in a proposal with Koudelka at TUG as the PI, and which was approved by ASA in 2006. This was the birth of the first satellite built in Graz (and Austria): BRITE-AUSTRIA, also called TUGSAT-1. The link to MOST is highlighted in a sentence of the proposal: BRITE-AUSTRIA will extend and supplement the spectacularly successful Canadian microsatellite MOST into the domain of nanosatellites.

As the Austrian BRITE's were accepted for funding, Slavek Rucinski felt that Poland (his country of birth) with its rapidly improving economy should join. When the Canadian part of the project appeared to be in limbo due to CSA dragging its heels regarding funding (from 2006 until 2011), he started pushing his colleagues and former students in Poland to follow the Austrian example. Aleksander Schwarzenberg-Czerny (Copernicus Astronomical Center, Warsaw, CAMK and former PhD student of Rucinski) was able to obtain funding for two BRITE satellites at the end of 2009 and, hence, he provides the fourth root of BRITE-Constellation.

The pressure on the Canadian Space Agency (CSA) increased considerably, after Austria funded UNIBRITE and BRITE-AUSTRIA, and after Poland funded BRITE-HEWELIUSZ and BRITE-LEM. Finally, CSA accepted in 2011 the two Canadian BRITE's (former CanX-3): BRITE-TORONTO and BRITE-MONTREAL.

In this way, BRITE-Constellation was born with six satellites.

### 3. BRITE-Constellation

The goal of BRITE-Constellation [34] was to provide high-precision photometric monitoring of very bright ( $\lesssim 4$  mag) stars in two optical wavelength bands (colours), that is, blue and red, and for up to six months, the maximum feasible time in an affordable low-Earth orbit. Various concepts have been discussed and finally a single telescope, optimized for a given passband was chosen with no moving elements on board, thus reducing risk, but which required one spacecraft per filter.

The proceedings of the First BRITE Workshop [35] provide an overview to the technical and scientific issues, which were discussed and decided before launch in 2013. The situation of the six (five active) components of BRITE-Constellation after launch (Table 1) are described in Weiss et al. [36], Deschamps et al. [37], Koudelka et al. [38] and various aspects of BRITE-data reduction in Pablo [39], Popowicz et al. [40], Popowicz [41].

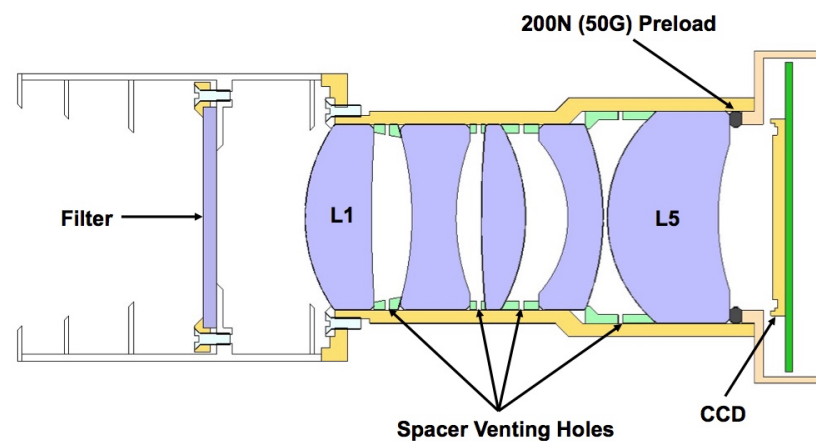
**Table 1.** Launch and orbital information for the BRITE nanosats. BRITE-MONTRÉAL did not separate from the launch vehicle and is not operational. The red filter covers 550–700 nm, and the blue filter 400–450 nm.

Owner	Name	Filter	ID	Launch Date	Orbit (km)	Period (min)
Austria	UNIBRITE	red	UBr	25 Feb. 2013	781 × 766	100.37
	BRITE-AUSTRIA	blue	BAb	25 Feb. 2013	781 × 766	100.36
Poland	BRITE-HEWELIUSZ	red	BHr	19 Aug. 2014	612 × 640	97.10
	BRITE-LEM	blue	BLb	21 Nov. 2013	600 × 900	99.57
Canada	BRITE-TORONTO	red	BTr	19 June 2014	629 × 577	98.24
	BRITE-MONTRÉAL	blue		19 June 2014		n/a

Conferences were organised almost every year to discuss updates and new aspects of the mission. Most importantly, they allowed for vivid scientific discussions which helped to shape the focus of BRITE-Constellation. The first science conference took place in 2015 in Gdańsk, Poland, one year later in Innsbruck [42], and in 2017 at Lac Taureau, Canada. The conference in Vienna “Stars and their Variability, Observed from Space-Celebrating the 5th Anniversary of BRITE-Constellation” in August 2019 provided the most recent status report [43].

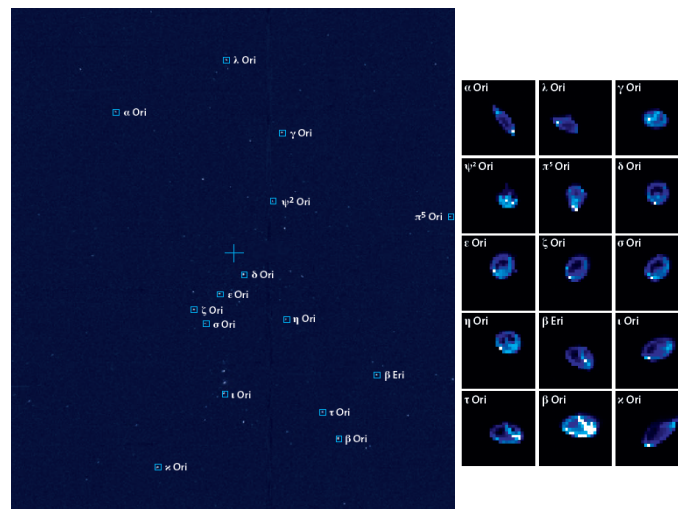
### 3.1. Instrumentation

The BRITE instruments consist of a multi-lens telescope with an aperture of 3 cm, optimised for the red (550–700 nm) or the blue (400–450 nm) wavelength range (Figure 4, red design). The unvignetted field of view (FOV) is about  $24^\circ$  in diameter and the optics were chosen to provide slightly out-of-focus stellar images for improved S/N, an experience acquired from MOST. For the two Austrian, the two Canadian and the blue Polish instruments a 5-lens system was developed. The red Polish instrument (BHr) has a four-lens design, which results in a shorter telescope, but with a smaller FOV of  $20^\circ$ . A baffle in front of each telescope reduces off-axis stray-light from bright sources, including the Sun, Moon and Earth.



**Figure 4.** Camera scheme for the UNIBRITE and BRITE-Toronto red instruments with a nearly vignetting free field-of-view of  $24^\circ$ . The red or blue filters are placed at the entrance pupil of the 5-lens camera to assure a constant filter function over the entire FOV. The blue cameras have slightly modified lens radii and separations to optimise the image quality for the needed wavelength range. Source: SFL.

The same interline frame-transfer CCDs, a Kodak KAI 11002-M ( $4048 \times 2672$  pixels and  $9 \mu\text{m}$  pixel size) chip, are used for each BRITE. This is an off-the-shelf product which includes all read-out electronics and preamplifiers on a header board behind the chip. Attractive features, besides the modest price, is the low dark current at high temperatures ( $0^\circ$ – $30^\circ\text{C}$ ), which allows one to avoid a cooling system, and a low read-out noise and power consumption. This CCD has been successfully used on the ground in SBIG Cameras, but never in the radiation environment of space. In order to avoid pixel saturation, the CCD is positioned out-of-focus, which, together with the optical design, results in about 8-pixel-wide on-axis stellar images. Off-center images have a more complex shape, as is shown in Figure 5. The scale is about  $27''$ – $30''$  per pixel, increasing slightly towards the edge due to image distortion.

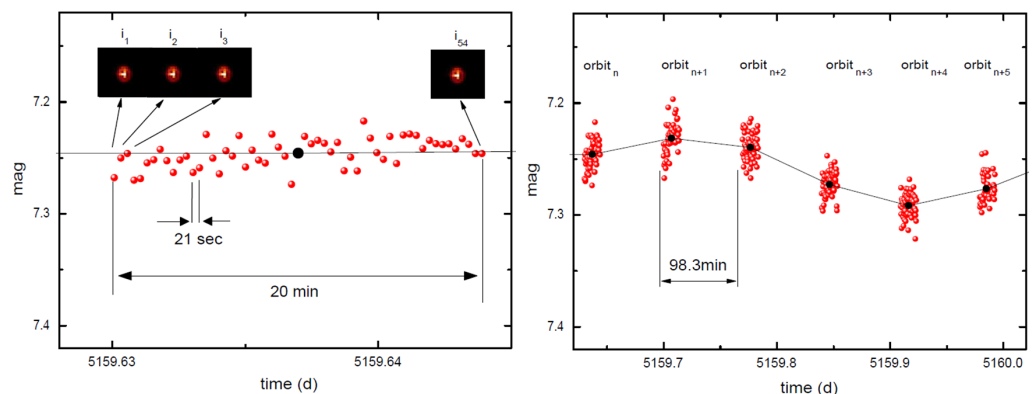


**Figure 5.** Full frame image of the Orion field taken with UniBRITE (UBr) in December 2013. The stars which have been selected for photometric time series are indicated. Subframes (24 × 24 pixels) which contain a full PSF, were stored in memory for a later download to the ground. Typical subframes in the center and close to the edge of the field are presented in the right panel.

### 3.2. Photometry and Data Processing

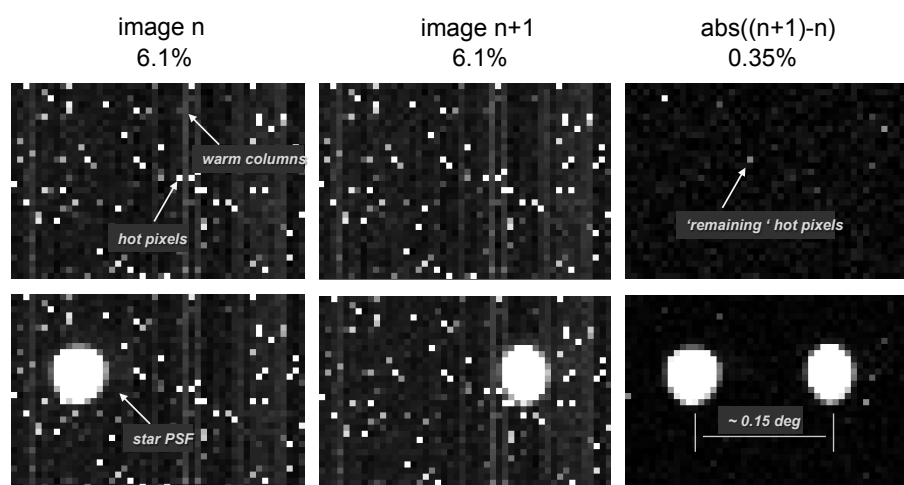
The BRITE mission requirements were set in 2005 such that the instruments shall observe a selected star-field for at least 15 min per orbit. Outside that time interval, scattered light from the Earth and Sun would be encountered. Data from up to 15 stars per field shall be collected for up to 100 days. In reality the BRITE satellites typically collect data from 24 to 28 stars during 20 to 40 min per orbit over a time base of about 160 days. The exposure times typically vary between 1 and 5 s and every 21 s subframes were read out. All functioning BRITE satellites were launched into low-earth polar orbits with periods close to 100 min.

Target fields can be occulted by the Earth during part of the orbit. After the field becomes visible again and its distance from the earth-limb exceeds a critical angle, the Attitude Control System (ACS) of the satellite re-points the star field in the camera FOV. To obtain top-quality photometry, the ACS must assure stable pointing of the PSF during the entire observing run close to the same pixels (flat-field exposures are not possible), which typically is achieved within 1.5' rms ( $\approx 3$  pixels). An example of such a photometric cadence is show in Figure 6. Whenever possible, a satellite setup was chosen, allowing one to observe a second field during an orbit, when the first field was invisible for the satellite.



**Figure 6.** A typical photometric sequence of 44 Cyg (Zwintz [44]), observed by BRITE-Toronto in the field during a single orbit (left) and the data sequence during six consecutive orbits (right), indicating intrinsic light variations.

After the first BRITE satellites (UBr and BAb) were launched and the first images were recorded, features appeared which were not present in the laboratory: pixels and even entire columns with increased dark (thermal) signal, that is, “hot pixels” and “warm columns” (Figure 7). These flaws were distributed over a significant fraction of the CCD, in the FOV as well as outside with no light access. The defects became stronger during successive weeks, even at the same CCD operating temperature. The signal of “warm columns” ranged from 100 to 500 ADUs above nominal background. One ADU corresponds at 20° C to 3.2 detected electrons. For a “hot” pixel the signal (even without illumination) is more than 100 ADUs above median background and it can even get close to saturation ( $\approx 1200$  ADUs). All BRITE satellites suffer from these radiation defects, believed to arise mainly from proton collisions, which accumulate over time and adversely affect the data reduction and quality.



**Figure 7.** Illustration of the chopping procedure. Top: empty rasters ( $24 \times 36$  pixel subsets of a frame). The left and middle raster was off-set horizontally by about  $0.15^\circ$ . Bottom: same as for top row, but with the telescope moved to a nearby star in the raster. Right column: absolute values of the raster differences. All images here were taken at about  $+20^\circ\text{C}$  operating temperature. The values on top of the upper row are the % of pixels which reveal a dark current higher than 100 ADU, compared to the median background of all pixels in the respective raster.

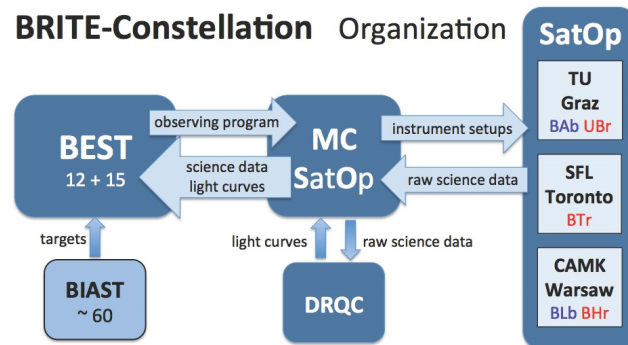
As is described in [40,41], a very efficient technique to overcome the mentioned detector flaws and to significantly improve the accuracy of the CCD photometry is the “chopping” technique, which was introduced to the observing procedure in November 2014 and installed in February 2015 as the default observing mode for all satellites. This mode replaced the previously used “stare” mode. In the chopping mode a satellite is shifted between exposures back and forth, so that for every second raster-image the star is positioned in the other part of the raster (Figure 7). Finally, the difference of two subsequent rasters contains essentially only information relating to the stellar brightness and all local background features are close to being eliminated.

Data reduction of all BRITE photometry is the responsibility of the Data Reduction and Quality Control (DRQC) team (see Section 3.3). The data corrected for, for example, the flux values with the CCD temperature and  $x$  and  $y$  pointing positions on the CCD, are archived and forwarded to the Principal Investigators (PI) for further de-correlation. De-correlation methods have been developed by Pigulski and documented as the “BRITE Cookbook”, which can be accessed together with the software code at <https://www.pta.edu.pl/pliki/proc/vol8/v8p175.pdf>. Examples of BRITE photometry are presented in Figures 6, 13–16, 18, 21 and 23.



### 3.3. Organisation and Operation

Organisation and operation of BRITE-Constellation relies on six interacting teams (Figure 8), which are:



**Figure 8.** Organisation structure of BRITE-Constellation. BEST: BRITE Executive Science Team, MC: Mission Control, SatOp: Satellite Operation, DRQC: Data Reduction & Quality Control, BIAST: BRITE International Advisory Science Team

- BEST (BRITE Executive Science Team) is the ruling body of BRITE-Constellation. It consists of two voting members per satellite, nominated by the three member countries (Austria, Canada and Poland) which funded the BRITE satellites. BEST elects additional non-voting experts, presently 15. BEST releases 6 to 12 months before a new observing campaigns starts a BRITE Observing Plan (BOP), which typically covers 12 to 14 months of operation. The BOP defines which satellite is assigned to which field and for how long (Figures 9 and 10). The rather long lead-time allows the PI's to organise supplementary observations from the ground or from space.
- MC (Mission Control) team is headed by Rainer Kuschnig (IKS, TU-Graz, formerly IfA Uni-Vienna) and is responsible for the execution of BOP by providing satellite orientation and instrument setup data. To ensure a maximum efficiency of BRITE-Constellation, a frequent quality control of all data generated with all active satellites is another core activity of MC. Such tests are applied at least twice a week and reported to BEST every second week. In case of problems, MC interacts directly with the corresponding satellite operator in charge.  
A very short turn-around time between data check and satellite operation is possible, because BRITE-Constellation observes “only” up to 60 stars during a campaign and basically a single person inspects the data nearly in real time. The obvious benefit is a fast response to unexpected stellar variability. The best and most outstanding example is the serendipitous data collection from Nova Carinae 2018. Almost instantly it was apparent that BRITE-Constellation had caught the nova days before it was discovered visually. Hence, this early volatile phase could be covered by BRITE-Constellation in an unprecedented manner, as is explained in Section 4.16.
- SatOp (Satellite Operation) teams are other key elements of the mission. Satellite operators are in charge of controlling the national spacecraft via the ground stations, of which one is in Austria at TU-Graz, one in Canada at SFL-Toronto and a third one in Poland at CAMK-Warsaw. However, in case of emergency, communication is possible from each of the ground stations to any satellite to ensure uninterrupted satellite control and data management. This was, and still is, usually required during harsh weather conditions at particular ground stations or during maintenance periods.
- DRQC (Data Reduction and Quality Control) is another core element of the mission. The data received from each BRITE satellite on a daily basis is delivered by SatOp to MC for a preliminary quality check. Once a campaign on a given field is finished, all raw data are ASCII formatted with a FITS-like header and made available to DRQC, which generates pipeline-reduced data files (supervised by Adam Popowicz, Silesian University of Technology, Gliwice) [40], and performs quality control (supervised by

Bert Pablo, AAVSO). The original data, the raw science data (ASCII) files and the time series datasets are then submitted to the BRITE Data Archive (maintained by Andrzej Pigulski, University of Wroclaw). Most of the archive can be accessed publicly, but some data are still protected for a limited time for the corresponding PIs. The BRITE Public Data Archive can be found at <https://brite.camk.edu.pl/pub/index.html>.

- BIAST (BRITE International Advisory Science Team) is an informal group of presently 60 scientists, who have already successfully proposed relevant observations and/or are planning this in the future. Hence, BIAST members have expertise in BRITE data, have published the results and can advise BEST in optimising the observing program.
- GBOT (Ground-Based Observing Team), which is headed by Konstanze Zwintz (U. Innsbruck), provides a platform for BRITE scientists and observers worldwide to support collaboration and to maximize the scientific output of BRITE-Constellation.

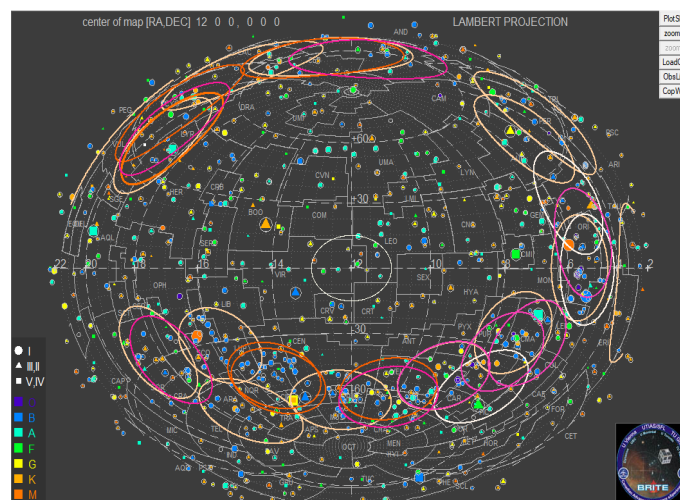


Figure 9. Sky map highlighting the fields observed thus far by at least one BRITE satellite.

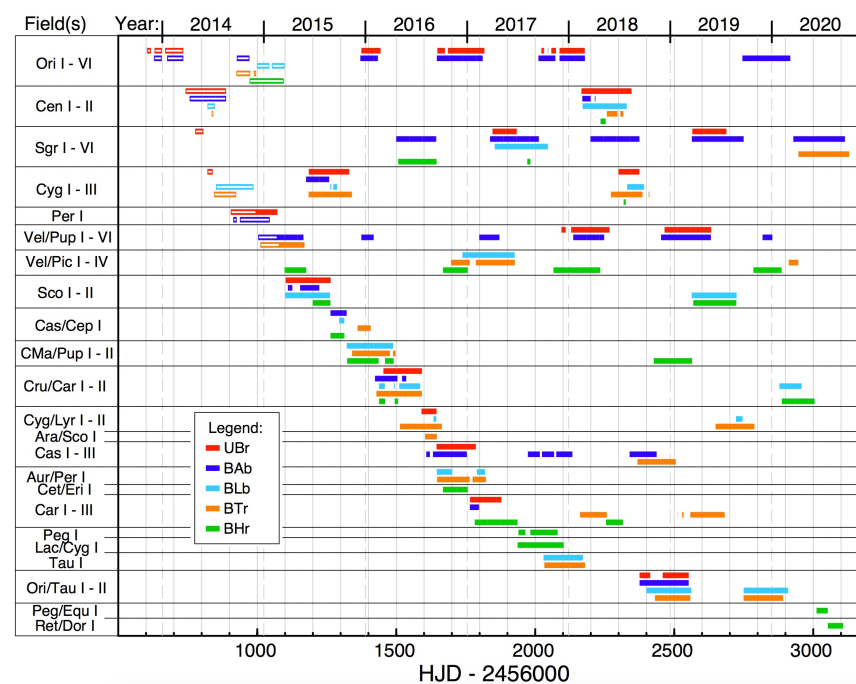


Figure 10. Temporal distribution of the observations of all five active BRITE satellites until the end of 2020. The data obtained in the stare and chopping observing modes are shown with unfilled and filled bars, respectively.

### 3.4. Present Status

The various star fields observed with various BRITE satellites since launch and until 2020 are presented in Figure 9. Which satellite observed a field in which period, either in chopping or stare mode, is indicated in Figure 10.

As of March 2021, 705 individual stars have been observed so far, often contemporaneously in two colours, and almost 6 million image-rasters of target stars have been produced. Most observations occurred in fields close to the Galactic plane, where the density of very bright stars in the FOV is high, allowing a proper choice of guide stars by the much less sensitive guiding telescope (Figure 9). Also many of the primary targets listed in the early BRITE proposals were located in this area, for example, the bright OB, B and Be stars in Orion, Carina, Centaurus or Sagittarius.

The observing strategy of BEST during the past eight years focused not only on stars of primary interest to the BRITE-community, like 6-month campaigns on hot, massive and intrinsically bright stars, but also to re-observe high profile targets essentially every possible season. The best examples are the brightest stars in the Orion field, which have been selected for the first campaign starting in December 2013 and which are currently being observed for the eighth time (Figure 10). These datasets are certainly jewels of the BRITE-Constellation legacy program.

Even though the early BRITE science program focused on O to B (including Be) type stars, it also includes now objects beyond this range in the HR diagram (Figure 12), which is indebted to wide field photometry, reaching by default many stars and of different type. For example, cool red-giants have been observed, although not originally considered a priority, but the first data analysis led already to a relevant publication. An excellent example is  $\beta$  Pictoris (Section 4.11). Finally it should be mentioned that TESS obtained data for stars which BRITE satellites observed simultaneously. An example was already given in Section 1 with  $\zeta$  Puppis.

For all BRITE satellites the nominal lifetime was two years. Hence, the still active satellites exceed this limit more than three times, which illustrates the high engineering quality. Nevertheless, BRITE-Constellation encountered technical problems described in the following.

The photometric accuracy is limited primarily due to stabilisation problems of BRITE satellites, but also by problems related to increasing CCD defects (Popowicz [45], Popowicz and Farah [46]). The development, e.g., of the normalised detector dark current with time is presented in Figure 11. Obviously, satellites with either a tungsten or a light weight borotron shield suffer significantly lower thermal noise increase compared to unshielded CCDs. Moreover, the sensors probably received different radiation doses during launch, as is indicated in Figure 11 by the onset of the linear approximations.

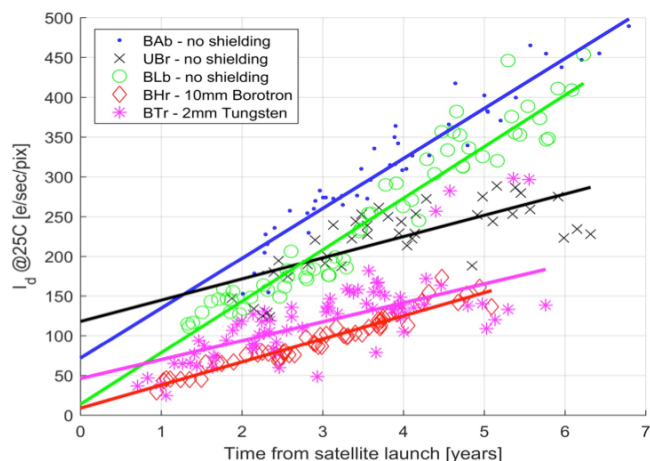


Figure 11. Temporal development of the CCD dark currents.

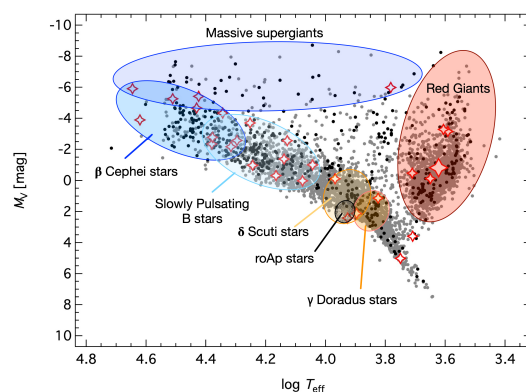
The status of individual BRITE satellites can be summarized as:

- BRITE-Toronto (BTr), is in good condition and produces among the best data, despite a significant amount of radiation damage. Primary target stars can be placed on the CCD where the background is least noisy.
- BRITE-Heweliusz (BHr), is working very well in general; some observing fields seem to cause problems for the pointing system, but usually alternative orientations of the field (different guide stars) can be chosen. It also has the least amount of radiation damage due to a better shielding of the CCD.
- BRITE-AUSTRIA (BAb) produces scientifically relevant data, even after more than eight years in orbit and an enhanced radiation environment. To obtain the best photometric consistency over the lifetime of BRITE-Constellation, this satellite has been assigned to observe every year essentially the same set of fields in Orion and Sagittarius.
- UniBRITE (UBr), was working well until June 2019, despite its high grade of radiation damage. However, it failed after that date and a failure analysis led by SFL and conducted by IKS TU-Graz concluded that one of the three reaction wheels seems to be damaged and cannot be used for stabilising the spacecraft. A repair concept is being developed.
- BRITE-Lem (BLb), worked well until April 2020 when it consistently failed to get into fine pointing. This is very likely due to a damaged reaction wheel. However more tests are still to be conducted to come to a firm decision.

In conclusion, presently three of the five functioning BRITE-Constellation satellites are still operational: BHr and BTr are producing very good data and BAb still useful photometry. BEST expects to continue the mission until at least in 2022, depending on unpredictable technical failures, for example, of the reaction wheels. Attempts to recover the other two BRITEs will continue.

#### 4. Key Results of the Mission and Scientific Highlights

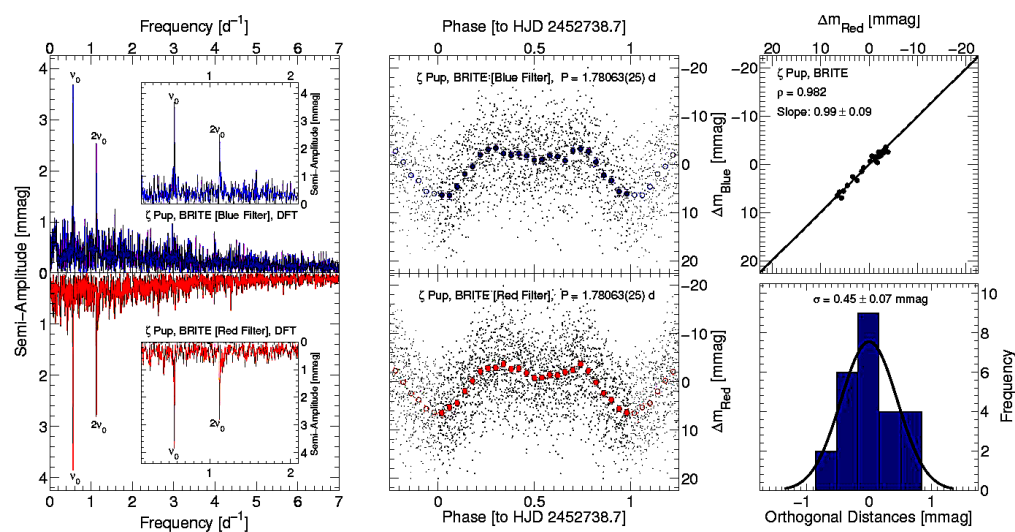
Since its launch BRITE-Constellation has obtained measurements for 705 individual targets in 60 currently completed fields (Figure 9) of which many overlap. A large fraction of the targets was observed in more than one field which yields total time bases of up to eight years for several stars (Figure 10). As of March 2021, 11.5% of all targets observed by BRITE-Constellation are included in one or more peer-reviewed publications. BRITE data of many other targets are still being actively analyzed and will be the topics of additional future papers. In the following, selected research highlights based on BRITE-Constellation data are presented, mostly sorted from most massive to least massive stars. The individual objects are also indicated in Figure 12.



**Figure 12.** HR diagram of the stars brighter than 6th mag in  $V$  (grey dots). Stars for which BRITE photometry was collected are shown by black dots. The objects discussed in Section 4 are marked as open red symbols where the larger symbol stands as a representation of the 23 red giants discussed in Section 4.15. Indicative instability domains for several types of pulsators are shown as colored ellipses. Be stars cover much of the  $\beta$  Cep and SPB domains

#### 4.1. The Link between Stellar and Wind Variability in Very Massive Stars

High-precision photometry of the runaway early-O-type supergiant  $\zeta$  Puppis (Figures 1, 2 and 13) revealed that a previously-proposed rotation period of 5.1 d is incorrect and the period actually is 1.78 d, which agrees much better with a model for the rotational evolution. Figure 13 also indicates that the large, real scatter beyond the 1.78 d modulation, is probably due to stochastically varying short-lived bright regions in the photosphere arising in a subsurface convection zone, which led to clumps in the wind. An alternative supposition is that the stochastic variability arises from gravity waves at the internal radiative/convection border. This is supported by hydrodynamic simulations showing gravity waves causing stochastic variability in the photospheres of main sequence OB stars (Bowman et al. [47]).



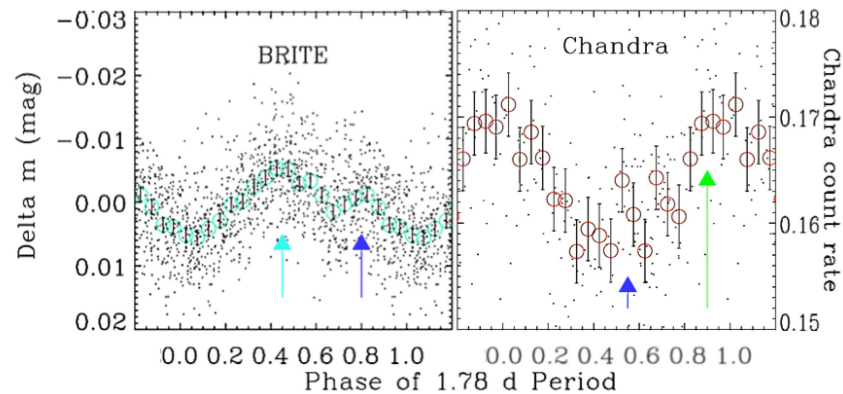
**Figure 13.** Left: Fourier transform of the red and blue 2014/15 BRITE photometry of  $\zeta$  Puppis (see Figure 10 for VelPup I–VI runs). Middle: Corresponding rotation light curve ( $P = 1.78$  d). Coloured points are 0.04 phase bins with  $1\sigma$  error. Note the large, real scatter, which could be due to stochastically varying short-lived bright regions in the photosphere which lead to clumps in the wind. Right: Comparison diagram for the phased blue and red light curves (top), and distribution of orthogonal distances with a Gaussian fit (bottom). (Figure 5 of Ramiamanantsoa et al. [48]).

The top diagram in the right column of Figure 13 shows that both kinds of bright spots show the same variability amplitude in the BRITE blue and red filters, implying insensitivity to the expected hotter nature of the spots compared to their adjacent areas in the stellar photosphere. The reason for this is that the Rayleigh-Jeans tails of the stellar emission spectrum are sampled at significantly longer wavelengths, compared to the UV maximum peak. The bottom diagram in the right column is consistent with the photometric precision of the data.

The findings yielded by the 2014/2015 observing campaign on  $\zeta$  Puppis may be an important resolution of a long-standing puzzle indicating subsurface convection as the main source of the two types of wind variability (quasi-periodic co-rotating interaction regions-CIRs-and stochastic clumps), which previously was not considered possible in such hot stars.

After this study of  $\zeta$  Puppis, parallel observations were obtained in 2018/19 using BRITE in the optical and Chandra in X-rays (Nichols et al. [49]). Both satellites confirm a 1.78 d period (Figure 14), which is thought to be the result of bright photospheric spots driving CIRs in the stellar wind, with the X-rays arising somewhat further out in the wind, where the CIR shock is strongest. Alternatively, as noted above, the stochastic component of variability could arise from gravity waves arriving from a much deeper zone.





**Figure 14.**  $\zeta$  Puppis observed in the visible with BRITE and in X-rays with Chandra, folded with the period of 1.78 d. The multi-wavelength light curve behaviour presumably illustrates the effects of Corotating Interaction Regions. The cyan arrows indicate the primary and the blue arrows the secondary maximum. There is a significant shift in the times of maximum due to a large delay or a smaller shift but mismatch in which is primary and secondary maximum (Figure 3 of Nichols et al. [49]).

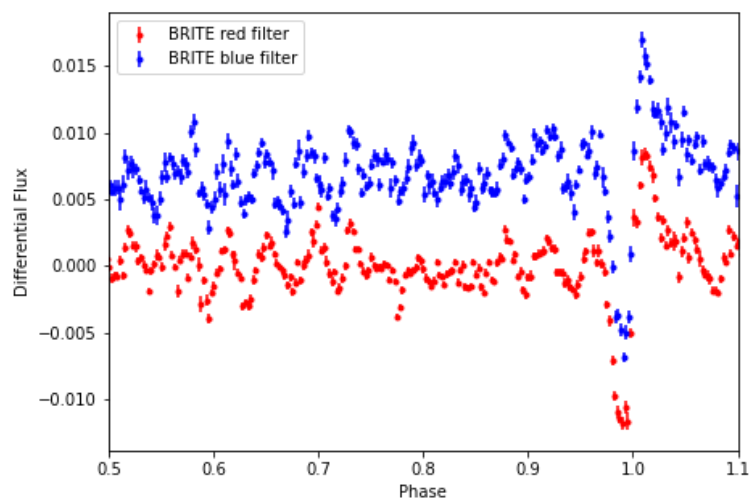
A very recent investigation was made on about 60 bright galactic Wolf-Rayet stars using combined data sets from MOST, BRITE and TESS by Lenoir-Craig et al. (submitted to ApJ and in [50]). Fourier analysis of the light curves reveals an important trend of enhanced stochastic variability at low frequencies ( $\lesssim 1 \text{ cd}^{-1}$ ) with the spectrally-modelled hydrostatic-core temperatures ( $T^*$ ), much like a preceding ground-based spectral variability study by Chené et al. [51,52]. Both studies support the idea that the stochastic variability seen in all WR stars arises in clump formation and propagation in their strong winds, such that, surprisingly, hotter WR stars with faster winds show less variability and hence less clumping. This can be explained by the triggering of the clumps in subsurface convective zones that are deeper and stronger in cooler WR stars. This may or may not conflict with the heretofore theory of clump formation by wind instabilities, which are expected to be stronger in hotter, faster WR winds.

Other targets with similar science relevance are WR 40 (WN8h; Ramiaramanantsoa et al. [53]), V973 Sco (O8Iaf; Ramiaramanantsoa et al. [54]) and  $\gamma^2$  Vel (WC8+O7.5III-V; Richardson et al. [55]). They were among those prominently observed by BRITE-Constellation during several runs and helped to investigate the dynamics of winds and their relation to variations occurring at the stellar (hydrostatic) surface.

#### 4.2. The Heartbeat of Stars: $\iota$ Orionis and $\epsilon$ Lupi

Heartbeat stars are a class of eccentric binaries which are characterized by tidally excited oscillations (TEO) with distinct amplitude changes at periastron. They are uniquely interesting for the study of massive stars, because they allow for full binary solutions without eclipses and provide access to asteroseismology of objects where pulsation is rare. Using BRITE-Constellation, the well-studied binary system  $\iota$  Ori (O9III+B1 III/IV) was the first massive star ever in which TEOs were discovered, and which opened a whole new avenue to studying massive star interiors (Pablo et al. [56]). The data in Figure 15 are phased to periastron (phase = 1.0, with  $P = 29.13376 \text{ d}$ ) and binned to 0.0025 in phase.

Another unique heartbeat star discovered with BRITE-Constellation was  $\epsilon$  Lupi. This system is the only known doubly magnetic massive binary (Shultz et al. [57]). Pablo et al. [58] were able to determine masses and radii despite an orbital inclination of  $\approx 20^\circ$ . This allows one to explore the interesting interplay between magnetism and tidal effects in the evolution of such a system.



**Figure 15.** Binned and phased data of  $\iota$  Ori, obtained with BRITE-Constellation, covering two years. The data clearly show tidally excited oscillations, most prominently from 0.5–0.8 in phase, as well as a strong heartbeat signal (0.95–1.05 in phase). The blue points are shifted by a constant flux for clarity.

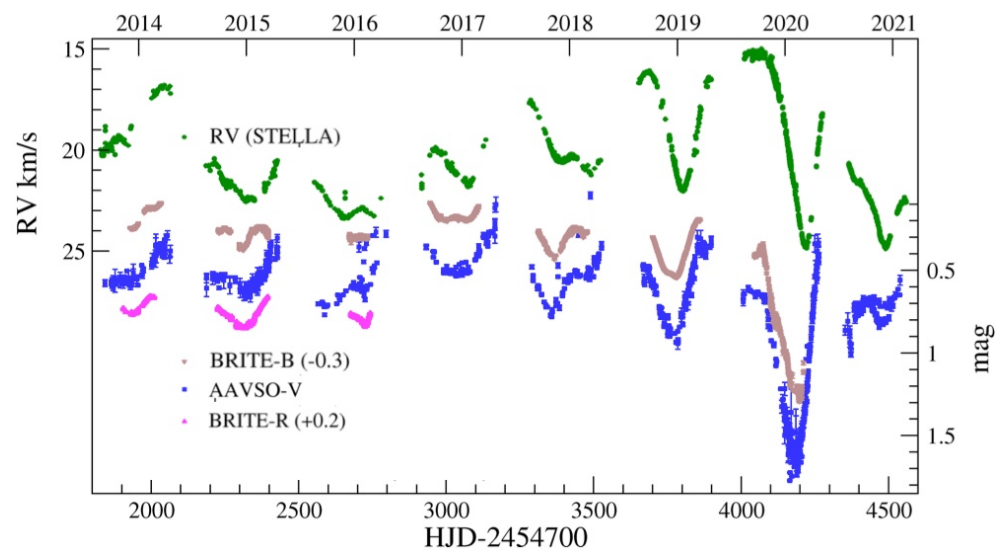
The value of BRITE heartbeat stars also extends to the upper reaches of the HR diagram with the enigmatic and highly eccentric binary system  $\eta$  Car, although the length of the period combined with mass loss have made it difficult to characterize any heartbeat signal at periastron. Using two separate BRITE observations, Richardson et al. [59] were able to confirm oscillation frequencies, which appear to be stable over the past four decades (van Genderen et al. [60], Sterken et al. [61]). These frequencies share many similarities with TEOs, though this identification will need more data to confirm.

#### 4.3. The Riddle of Betelgeuse

The red supergiant Betelgeuse is not only one of the biggest stars in the sky, but also one of the most puzzling. Long-term photometry and radial velocity studies reveal semi-regular stellar pulsation periods of 420 d, and possibly superposed by a cycle of 8.7 years (Goldberg [62], Dupree et al. [63], Smith et al. [64]). In comparison, Kiss et al. [65] report  $388 \pm 30$  days as a pulsation period and a  $5.6 \pm 1.1$  years cycle, using AAVSO-V data obtained almost during an entire century (1918–2006).

Curiously, its high apparent brightness makes Betelgeuse a difficult target for ground-based photometry, as big telescopes suffer from over-exposure. This gap is now filled with high-quality BRITE photometry (Figure 16), augmented with spectroscopic data obtained during more than 10 years at the STELLA robotic observatory, which is one of the biggest fully robotic telescopes worldwide (Strassmeier et al. [66]). Only automated observing procedures allow scheduling of almost daily visits of the same star, each lasting no longer than 5 min and stretching over more than a decade. More than 2000 individual, high-resolution spectra have been collected and automatically reduced.

As Figure 16 illustrates, the radial velocity variations follow in general closely the photometry, suggesting a physical link between photometric and radial velocity variations. A splitting of the main pulsation period into  $P \approx 420$  d and  $P \approx 335$  d, as seen in the RV-data, is proven beyond doubt by BRITE photometry, which provides the required cadence and precision. This is work in progress—adding another season will hopefully put these findings on solid grounds.



**Figure 16.** Comparison of light and RV variations of Betelgeuse. From top to bottom: STELLA RV data, BRITE-blue, AAVSO-V absolute photometry, and BRITE-red photometry. Error bars on BRITE magnitudes and on STELLA RV are too small to be visible.

During the grand dimming event in the 2020/21 season, an extraordinarily excursion of the photometry to the RV-data can be seen. The photometric amplitude by far outstretches the already high RV amplitude. An analysis of HST UV-data of this period (Dupree et al. [67]) hints to a big plume of dust being emitted from the surface of the star and subsequently drifting into the line of sight, thereby enhancing the photometric minimum.

Betelgeuse is approaching its end of life as a star, commonly believed to be a supernova progenitor. Last year's dimming event sparked estimates that an explosion may be imminent within the next 100,000 years. But observations and models are currently not refined enough to prove whether Betelgeuse will end in a type IIb, II-L, or II-P supernova (Meynet et al. [68]). Hence, new observations are needed to better estimate mass and rotation rate in order to pin down Betelgeuse's future path. BRITE-Constellation will participate in these campaigns.

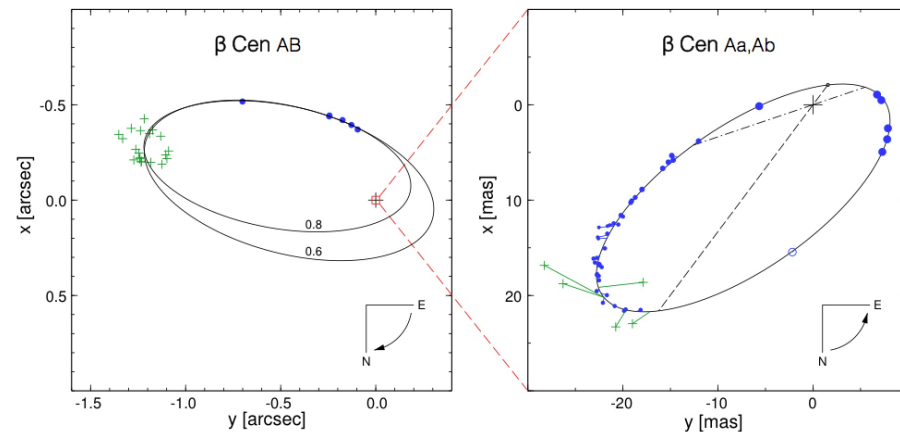
#### 4.4. Evolving Pulsation of the Slowly Rotating Magnetic $\beta$ Cephei Pulsator $\zeta^1$ CMa

$\zeta^1$  CMa is a remarkable magnetic early B-type star that is distinguished in several ways: it rotates extremely slowly ( $P_{\text{rot}} \sim 30$  y; Shultz et al. [69]), it is the only magnetic B-star known to exhibit detectable H $\alpha$  emission from a dynamical magnetosphere [69], and its optical and X-ray magnetospheric emission are modulated according to its  $\sim 0.2$  d radial pulsation period (Shultz et al. [69], Oskinova et al. [70]).

Building on work by Pigulski [71], Jerzykiewicz [72] and Shultz et al. [69], BRITE-Constellation photometry (BLb, BHr, BTr) of  $\zeta^1$  CMa was employed by Wade et al. [73], as one of the most recent anchor points to monitor the evolution of its pulsation period. Combining over one century of photometric and radial velocity monitoring, they concluded that the period evolution of  $\zeta^1$  CMa consists of a secular period lengthening of roughly 0.3 s/century that can be satisfactorily understood as a consequence of expansion due to stellar evolution. An additional period evolution—more rapid and of lower amplitude—remains unexplained, and the authors speculate that it may be a consequence of rotational modulation or evolution that is restricted to relatively rapid, short-term episodes, rather than uniform long-term changes. Binarity can be ruled out, because the corresponding RV variations would have been easily detected.

#### 4.5. The Triple System $\beta$ Centauri

Massive stars, with initial masses greater than  $8 M_{\odot}$ , are among the least understood, but they are extremely important, because they produce the majority of heavy elements. A fascinating BRITE-Constellation target is the triple system  $\beta$  Centauri (Figure 17)—also named Agena—consisting of a massive binary ( $\beta$  Cen AaAb: B1 II and B1 III) with an eccentric orbit and a more distant and 3 mag fainter companion, also of B-type (Pigulski et al. [74]).



**Figure 17.** The triple system  $\beta$  Centauri, with two example orbits (eccentricity of 0.6 and 0.8). Adapted from Figures 1 and 2 of Pigulski et al. [74].

$\beta$  Cen B was discovered in 2011 as a magnetic star (Alecian et al. [75]). With 17 detected p and g modes, the close massive binary system becomes one of about a dozen known hybrid  $\beta$  Cep/SPB stars with such a rich frequency spectrum. Furthermore, its binarity provides a very precise determination of the masses of the components, but complicates seismic modeling, because the modes need to be safely assigned to one of the components, which—in addition—are relatively fast rotating.

The case of  $\beta$  Cen illustrates the potential of BRITE-Constellation data for the detection of rich-frequency spectra of small-amplitude modes in pulsating stars.

#### 4.6. Long-Period Oscillations in the $\beta$ Cephei Pulsators $\nu$ Eridani and $\theta$ Ophiuchi

Thanks to the long-term stability of BRITE, Handler et al. [76] detected several previously unknown long-period signals corresponding to gravity-mode oscillations of the  $\beta$  Cephei pulsator  $\nu$  Eridani. Daszyńska-Daszkiewicz et al. [77,78] demonstrated that present standard pulsation models cannot reproduce the observed frequency range of g-mode pulsations, which is likely due to shortcomings in the underlying stellar physics data, in particular of opacities.

Upon the detection of a large number of g-mode pulsations in the BRITE data of another  $\beta$  Cephei star,  $\theta$  Ophiuchi, Walczak et al. [79] arrived at an identical conclusion (with the caveat that a B5 companion star could be responsible for the g modes), namely that opacities need to be increased between 30% and 145% (!) in the range  $\log T = 5.06$ – $5.47$  to reproduce the observations. Obviously, the use of correct opacity data is important for modelling of all kinds of stars. Hence, the implied revision of these data impacts stellar physics in general.

#### 4.7. The Ellipsoidal SPB Variable $\pi^5$ Orionis

BRITE observations of the ellipsoidal variable  $\pi^5$  Orionis (Jerzykiewicz et al. [80]) revealed that the primary star belongs to the class of Slowly Pulsating B (SPB) stars. Within the modes of pulsation, there is a re-occurring splitting of twice the orbital frequency. This is interpreted as perturbation of nonradial pulsation modes by the equilibrium tide exerted by the companion. The behaviour of the two tidally disturbed pulsation modes

is largely consistent with axisymmetric dipole modes ( $l = 1, m = 0$ ). These findings have two important and interesting consequences:

- $\pi^5$  Ori is the first SPB star in which tidal perturbations have been identified and
- these perturbations facilitate the identification of nonradial pulsation modes. BRITE allowed a valuable proof-of-concept of mode identification to be carried out, which opened up tidal asteroseismology of SPB stars in multiple systems.

#### 4.8. Be Stars

The BRITE database is rich in Be-star observations because there are many bright Be stars and, for B-type stars, the blue- and red-sensitive BRITE satellites achieve roughly equal S/N, unless an extreme reddening is present. The combination of the frequency resolution and quality of BRITE observations over several seasons with the long-term behaviour documented by SMEI has achieved qualitatively new insights into the so-called Be phenomenon.

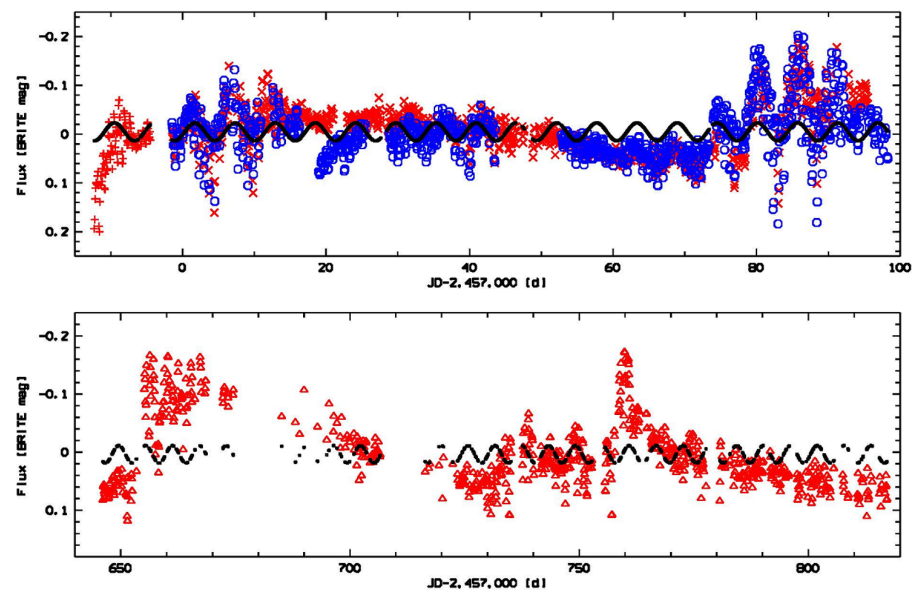
Two central questions about Be stars (see Rivinius et al. [81] for a review) are:

- (i) How do Be stars maintain their Keplerian accretion disks where the eponymous emission lines form and that, without regular replenishment, dissipate within a year?
- (ii) How have Be stars acquired their  $\gtrsim 75\%$  critical rotation? One way to explain the latter is mass transfer in a close binary. The former primaries often appear as hot, subluminal sdO stars that are challenging to detect even in UV spectra (Wang et al. [82]) and contribute little flux in the BRITE passbands. However, first photometric Doppler shifts derived from BRITE and SMEI data spanning 25 years have set an upper limit of  $\sim 1 M_{\odot}$  on the mass of a putative companion of  $\nu$  Pup (Baade et al. [83]).

BRITE-Constellation has been instrumental in confirming earlier suggestions that Be disks are fed by discrete mass-loss outbursts driven by the superposition of several low-order non-radial pulsation modes or by recently detected stochastically-excited pulsations, transporting angular momentum from the stellar core to the surface (Neiner et al. [84]). Although originally detected in H $\alpha$  line profiles of  $\mu$  Cen (Rivinius et al. [85]), optical photometry is a better tracer of outbursts because the V-band flux responds sensitively to varying amounts of ejecta causing electron scattering and free-bound recombination (Haubois et al. [86]). In fact, in  $\mu$  Cen, outbursts have up to 100 times higher amplitude than the underlying non-radial pulsation and can render the pulsations undetectable (Baade et al. [87]). In  $\eta$  Cen ([87]), 28 Cyg (Baade et al. [88]), and 25 Ori (Baade et al. [89]), BRITE found closely spaced NRP frequencies the difference between which corresponds to the repeat frequency of the outbursts. During an outburst, the combined amplitude of the involved non-radial pulsation modes grows nonlinearly, demonstrating that the outbursts are pulsation powered far beyond mere mode beating. Hierarchically nested frequency groups can drive repetitive outbursts on timescales from weeks to years (Figure 18), and the frequency groups typical of Be stars can be understood as difference frequencies (g0), non-radial pulsation frequencies proper (g1), and sum/harmonic frequencies (g2) ([89]). So-called Štefl frequencies first found in emission lines (Štefl et al. [90]) probably are orbital frequencies in the innermost inhomogeneous disk (Baade et al. [87]).

For shorter timescales/lower amplitudes, TESS (Labadie-Bartz et al. [91,92]) has confirmed the correlation between increased non-radial pulsation amplitude and mean brightness. Similarly tight networks of selected non-radial pulsation frequencies do not seem to be known from other stars, and the outbursts may enable Be stars to escape an angular-momentum crisis possibly caused by the contracting core (Baade and Rivinius [93]). The detection of non-radial pulsation modes by BRITE (Borre et al. [94]) and TESS (Labadie-Bartz et al. [92]) has also terminated decades-long speculations that the best-known Be star,  $\gamma$  Cas, shows rotational variability due to a magnetic field (Smith and Henry [95]).





**Figure 18.** Blue (blue symbols) and red (red symbols) BRITE light curves of the Be star 25 Ori (cf., Baade et al. [89]) from 2014/15 (top) and 2016/17 (bottom). In either season, two outbursts separated by  $\sim 78$  d occurred which corresponds to the difference frequency of  $0.0129$  c/d between many pairs of non-radial pulsation modes. The black curves are a sine fit to the 2014/15 light curve outside the outbursts with frequency  $0.1777$  c/d which is another difference frequency in multiple non-radial pulsation frequency pairs. During the outbursts in 2014/15, the light is modulated with  $0.1777$  c/d, less clearly so in 2016/17. The change in mean magnitude after the outbursts is probably due to increased scattering and free-bound transitions in the subsequently dissipating ejecta.

#### 4.9. $\beta$ Lyrae: A Binary with a Hidden Component?

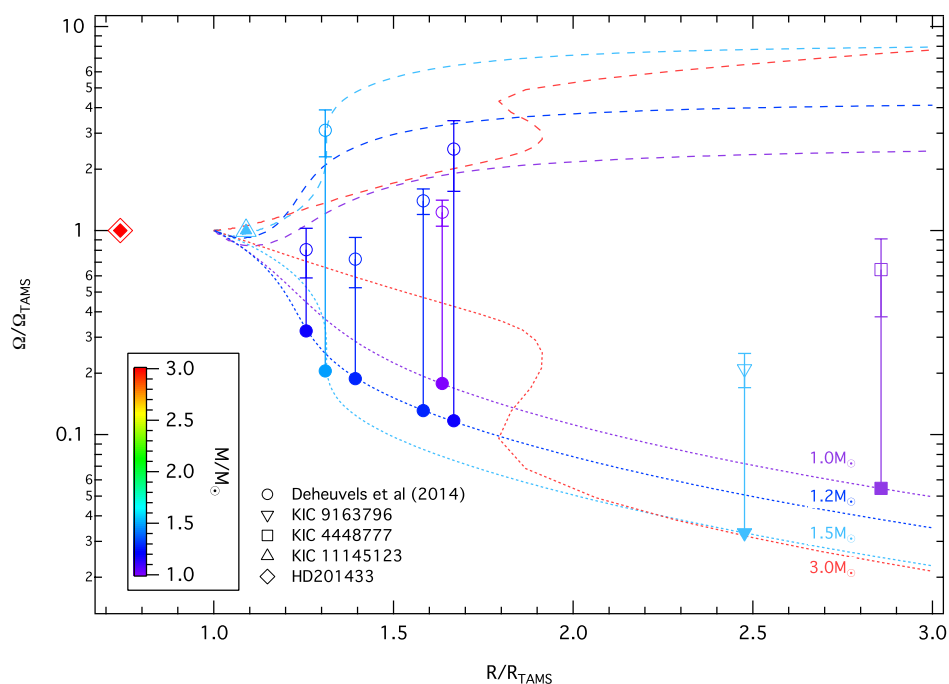
A highlight binary is  $\beta$  Lyrae, which consists of a B6-8II bright giant ( $3 M_{\odot}$ ) and an invisible, more massive companion ( $13 M_{\odot}$ ) producing the primary eclipses. The bright giant loses mass to the more massive companion at a rate that induces a fast period change of 19 s per year. There were no previous studies of the intrinsic variability of the  $\beta$  Lyrae system available which were credible, sufficiently continuous, and uniform, because of the day-gaps in ground-based observations, which coincided with the prevalent time-scales of the intrinsic variability in this 12.9-day orbital-period binary.

The BRITE data extending over slightly more than 10 full orbital revolutions of the binary provided the first usable time series, reaching substantially beyond the intrinsic time scales and permitting utilisation of tools well developed for studies of variability of active galactic nuclei and quasars. Analysis of the BRITE time series shows typically three to five instability events per binary orbit, showing a slightly stronger serial correlation than the red noise (Rucinski et al. [96,97]). The two-parameter Damped-Random-Walk (DRW) model of the fluctuations (Kelly et al. [98], Zu et al. [99]), characterised by the red-noise spectrum at time scales shorter than the de-correlation time scale  $\tau$  and white noise at longer time scales, agrees very well with the data.

The fluctuations are characterised by the amplitude of the stochastic signal of 1.3%, expressed relative to the maximum flux from the binary, while the de-correlation length of the random disturbances is characterised by a typical value of  $\tau = 0.88$  days. The invisible companion is the most likely source of the instabilities. Unexpectedly, the time scale of the intrinsic variability—most likely associated with the thermal time scale of mass-transfer instabilities—appears to follow the same dependence on the mass of the accreting object as is observed for active galactic nuclei and quasi-stellar objects, which are five to nine orders of magnitude more massive than the  $\beta$  Lyrae torus-hidden component.

#### 4.10. HD 201433—A Rosetta-Stone SPB Star in a Multiple System

Rotation is a still incompletely understood key process of stellar evolution (Aerts et al. [100]). If stars locally conserved angular momentum, their cores would spin up and the surviving compact objects would spin much faster than is actually observed. This implies that present standard models are incomplete and miss essential processes and correct timescales. A first step towards solving this problem is to detect how angular momentum is distributed inside stars, as a function of various parameters including age. Prime candidates for such studies, and more easily understood than B-type stars, are subgiant and red giant stars, as they convey the rotational history of the earlier stages of evolution and pulsate with mixed p/g modes that carry information about the deep stellar interior, as is argued in Kallinger et al. [101] and illustrated in Figure 19.



**Figure 19.** Mean core (dashed lines) and envelope (dotted lines) rotation rate during the evolution of YREC models (from the TAMS to the RGB) with various masses (colour coded) assuming local conservation of angular momentum and rigid rotation on the main sequence. The rotation rate and stellar radius are given relative to their respective values on the TAMS. The filled symbols correspond to the relative envelope rotation rates of various stars with a given mass and radius. The core rotation rate (open symbols) is determined from this value and the observed core-to envelope rotation gradient (Figure 19 of Kallinger et al. [101]).

BRITe-Toronto observed in 2015 the SPB star HD 201433 continuously for 156 days [101]. The peaks in the Fourier spectrum of the BRITe observations turned out to be broader than expected, which triggered the development of a new Bayesian-based frequency determination technique with a resolution beyond the formal Rayleigh-criterion. As a proof, three rotationally split triplets are identified in the nearly half-year long BRITe-data, with central frequencies and splittings agreeing well with those extracted from the nearly 8 years of SMEI observations.

A science highlight of the HD 201433 BRITe-photometry is a trend of splitting becoming more common towards longer periods, which implies a non-rigid internal rotation profile, as is elaborated in [101]. For a detailed investigation, a dense grid of MESA models [102,103] and their non-adiabatic pulsation modes were computed by Kallinger et al. [101]. Using classical  $\chi^2$  techniques and other statistical methods, a representative model ( $3.05 M_{\odot}$  and  $2.6 R_{\odot}$ ) was identified that reproduces best the observed frequencies.

The pulsation modes that are accessible to the seismic analysis probe the radiative envelope of HD 201433 from the boundary of the convective core at about  $0.11 R_*$  up to about  $0.98 R_*$ . The Bayesian analysis of various rotation profiles provides strong evidence for a slowly ( $292 \pm 76$  d) and rigidly rotating envelope, topped by a thin and significantly more rapidly rotating surface layer, which covers about the outer 4% of the radius (Figure 19). In conclusion, BRITE-Constellation data provide strong evidence for non-rigid internal rotation in a main-sequence star, which still is rarely presented in the literature.

#### 4.11. The Young Star $\beta$ Pictoris and Its Exoplanetary System

Exoplanet properties crucially depend on their host star's parameters. The  $\beta$  Pic system includes a wide, dense circumstellar disk that is seen edge-on and two giant gas planets ( $\beta$  Pic b and c) that are only grazingly eclipsing the host star. BRITE-Constellation data have been used to search for a transiting planet. This puts limits on the  $\beta$  Pic system, as possible planets must be larger than  $0.6$  ( $0.75, 1.0$ )  $R_{\text{Jupiter}}$  for periods of less than 5 ( $10, 20$ ) days (Lous et al. [104]).

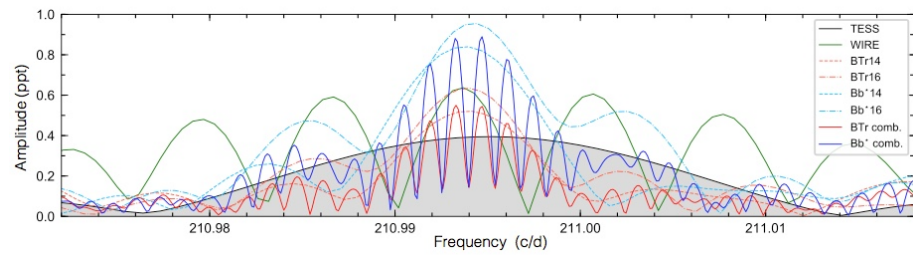
Furthermore, the predicted transit of the Hill sphere of  $\beta$  Pic b triggered an international observing campaign in 2017–2018 including the BRITE-Constellation nanosats. No dimming caused by the Hill sphere transit was observed in any of the involved photometric instruments, where the precision of the BRITE photometry would allow detection of a drop in intensity by only 0.5% in the time of interest (Kenworthy et al. [105]). In the spectroscopic observations, some signs of the Hill sphere transit have been detected (e.g., in the Ca II H & K lines) illustrating that the material in the planet's Hill sphere is not sufficiently dense to dim the stellar light enough to be photometrically detected from the ground. In addition, in 1981 anomalous fluctuations of the flux coming from the  $\beta$  Pic system were originally interpreted as being caused by foreground material that transited the stellar disk. Recently, based on the observations conducted within the  $\beta$  Pic Hill sphere transit campaign, Kenworthy et al. [105] showed that this 1981 event did not originate from the transit of a circumplanetary disk.

The high-quality BRITE-Constellation photometry for  $\beta$  Pictoris obtained since 2015 provided crucial constraints on the properties of the exoplanet host star itself (Zwintz et al. [106]). The first asteroseismic analysis using multi-color space photometry yielded a precision of 2% in mass and radius for  $\beta$  Pictoris, determined the inclination angle to be  $89.1^\circ$  (which agrees with the inclination angle of the disk of  $88.1^\circ$ ), and identified the 15 pulsation frequencies as three  $\ell = 1$ , six  $\ell = 2$  and six  $\ell = 3$  p-modes.

#### 4.12. The roAp Star $\alpha$ Cir

$\alpha$  Cir is the brightest rapidly oscillating (roAp) star with a magnetic field. It was discovered in 1981 by Kurtz and Cropper [107] and since then, many publications dealt with photometric and spectroscopic properties, including the magnetic field (see, e.g., Holdsworth and Brunsden [108] and Weiss et al. [109,110]).

$\alpha$  Cir is a text-book illustration for an advantage of nanosatellites dedicated to photometry (e.g., Weiss [19]), as they allow one to observe stars over a long time span. Even if the accuracy of individual data points is inferior to that of larger instruments, long observations of targets result in more accurate frequency spectra. Figure 2 of [110] presents light curves observed by five different satellites with apertures ranging from 3 cm (BRITE-blue) to effective 10 cm (TESS) and filter bandwidths of 55 nm and 400 nm, centred on 425 nm and about 800 nm, respectively, (see Table 1 of [110]). The larger the aperture and filter bandwidth, the more accurate the photometry, but if frequency-resolution is important, the picture changes drastically in favour of data obtained over 3 years even with a smaller aperture telescope (Figure 20).



**Figure 20.** Fourier amplitude spectra of the TESS, WIRE and BRITE photometry, centred on the main pulsation frequency ( $f_1$ ) of  $\alpha$  Cir. BTr14, BTr16, Bb\*14, and Bb\*16 are the red and blue BRITE data, obtained during the years 2014 and 2016, respectively. Bb\* represents the combined blue data obtained with BRITE-Austria and BRITE-Lem. The BRITE-blue amplitudes are divided by two (!) for better comparison with the other data (adapted Figure 6 of Weiss et al. [110]).

Combining the times of maximum from BRITE-red and WIRE data, results in  $f_1 = 210.993264(5) \text{ d}^{-1}$ , which is, with an error in the corresponding period of 0.01 msec, the most accurately determined dominant pulsation period of any roAp star to date. The main pulsation frequency ( $f_1$ ) can be identified with an  $\ell = 1$  mode, and two additional frequencies likely come from two consecutive radial  $\ell = 0$  modes [110].

At least three surface spots can be identified for  $\alpha$  Cir; the TESS data even suggest a fourth spot. The best-fit (minimum  $\chi^2$ ) set of parameters differs significantly from that inferred from the marginal distributions of the parameters, which hints at a noticeable skewness of the probability distribution of the Bayesian photometric imaging in the considered ten-dimensional configuration space. Obviously, spot latitudes are less well determined than longitudes, as expected. To our knowledge, this is the first time that Bayesian-based evidence of models differing in the number of spots has been quantitatively determined [110].

#### 4.13. $\beta$ Cas: The First $\delta$ Scuti Pulsator with a Dynamo Magnetic Field

One of the cooler BRITE-Constellation targets showing pulsations and a magnetic field is the F2 type star  $\beta$  Cas, which is also one of the objects in the BRITE legacy fields (Zwintz et al. [111]).  $\beta$  Cas is quite an unusual star in several aspects:

- (i) It shows only two independent  $\delta$  Scuti type p-mode frequencies. As  $\delta$  Scuti stars are usually known to show up to hundreds of individual frequencies, this challenges the asteroseismic interpretation. Why only two frequencies can be detected with a total time base of over 2.5 years is still unclear.
- (ii)  $\beta$  Cas is one of the few  $\delta$  Scuti stars known to date to show a measurable magnetic field at all [111]. The three other magnetic  $\delta$  Scuti stars are HD 188774 (Lampens et al. [112]),  $\rho$  Pup (Neiner et al. [113]) and HD 41641 (Thomson-Paressant et al. [114]).
- (iii) Additionally, the magnetic field structure of  $\beta$  Cas is quite complex and almost certainly of dynamo origin. One may speculate that the presence of this dynamo field is related to the unusual lack of numerous  $\delta$  Scuti frequencies.

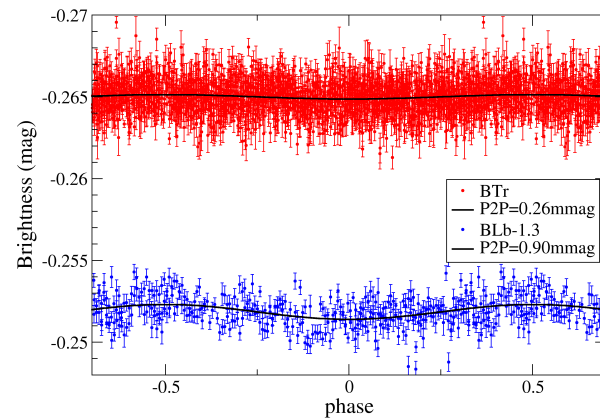
All this makes  $\beta$  Cas a powerful test bench for modelling of dynamo processes in thin convective envelopes of F-type stars.

#### 4.14. Rotation, Pulsation, Orbits and Eclipses in the Constellation of Auriga

The Auriga field is an excellent example of an arrangement typically chosen for observations with BRITE-Constellation. One or two key targets determine the orientation of a BRITE satellite and in the same field additional targets with a large mass-range maximise the science output.

Rotation and pulsation periods across the Hertzsprung-Russell diagram are of top priority for understanding stellar activity as a function of time. Continuous photometry with up to three BRITE satellites was obtained for 12 targets, primarily in the Aur/Per I field, and subjected to a period search (Strassmeier et al. [115]). The bright active star, Capella,

was found to be constant in the red bandpass with an rms of just 1 mmag over 176 d, but showed a  $10.1 \pm 0.6$  d periodicity in the blue, which is interpreted to be the rotation period of its active and hotter secondary star (Figure 21). Its position in the Hertzsprung gap suggests ongoing changes in its internal structure. It is expected that this has a profound impact on the visible surface and can explain its fast rotation.



**Figure 21.** Phase plots for the red (**top**) and blue data (**bottom**) with the best-fit 10.1 d period for Capella. The blue data are dominated by the hotter G0 component while the red data are dominated by the cooler G8 component. The rotation period of the cool component is near the orbital period of 104 days (adapted Figure 3 of Strassmeier et al. [115]).

Results for the other targets in Auriga include:

- (i) The main pulsation period of the F0 supergiant  $\epsilon$  Aur is detected by a multi-harmonic fit of the 152-day long light curve. This is noteworthy, because the RVs observed contemporaneously with the Stella spectrograph revealed a clear 68 d period. Although the light curve showed two minima separated by 74 d, a single period of that duration would not fit the data adequately. These RVs indicated that the (stellar) disk-integrated pulsations seem to revert when maximum or minimum light is reached, that is, the star is apparently most contracted when brightest and most expanded when faintest.
- (ii) An ingress of an eclipse of the  $\zeta$  Aur binary system was covered and a precise timing for its eclipse onset derived. We obtained a possible 70 d period from the outside-eclipse light-curve fits of the proposed tidally-induced, nonradial pulsations of this ellipsoidal K4 supergiant.
- (iii)  $\eta$  Aur was identified as an SPB star with a main period of  $1.289 \pm 0.001$  d. Five more periods are seen in the BRITE photometry and three of these are also seen in the RV data. The amplitude ratios as well as the phase lags between brightness and RV periods reflect those expected from low-degree gravity modes of SPB stars.  $\eta$  Aur is, thus, among the brightest SPB stars known.
- (iv) Rotation of the magnetic Ap star  $\theta$  Aur is easily detected by photometry and spectroscopy with a period of  $3.6189 \pm 0.0001$  d and  $3.6177 \pm 0.0006$  d, respectively. The RVs of this star show a striking non-sinusoidal shape with a large amplitude of  $7 \text{ km s}^{-1}$ , which is likely due to the line-profile deformations from the inhomogeneous surface distribution of its chemical elements. Such a non-sinusoidal shape likely explains the small period difference and suggests that the two periods are actually in agreement.
- (v) Photometric rotation periods are also confirmed for the magnetic Ap star IQ Aur of 2.463 d and for the solar-type star  $\kappa^1$  Cet of 9.065 d, and also for the B7 HgMn giant  $\beta$  Tau of 2.74 d. The latter remains uncertain because it was reconstructed only with the very small amplitude of 0.54 mmag.
- (vi) Revised orbital solutions are derived for the eclipsing SB2 binary  $\beta$  Aur, which replaces the initial orbit from 1948, and for the RS CVn binary V711 Tau for which a spot-corrected orbital solution was achieved. The two K giants  $\nu$  Aur and  $\iota$  Aur are found



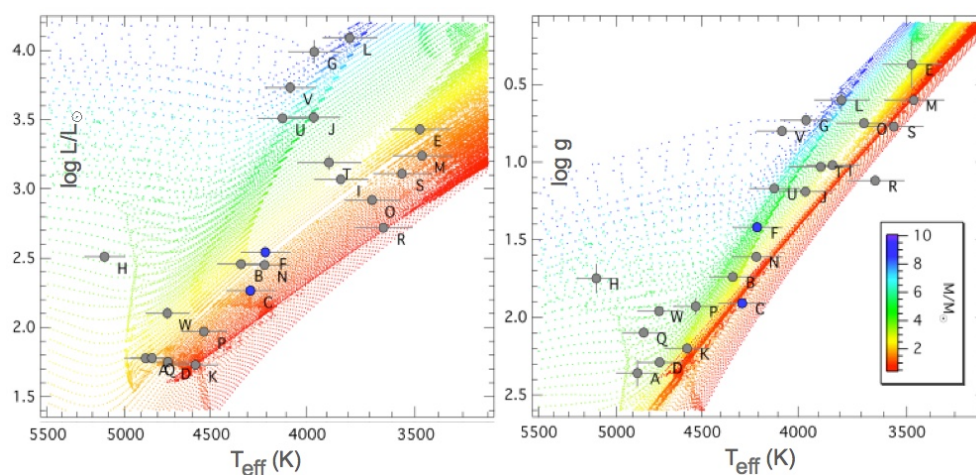
with long-term trends in both the light curve and the RVs.  $\nu$  Aur could be a long-period eccentric SB1 system with a low-mass companion for which a provisional orbital solution is predicted with a period of 20 yr and an eccentricity of 0.7. The RV variations of the hybrid giant  $\iota$  Aur are of even lower amplitude ( $0.7 \text{ km s}^{-1}$ ) but shorter period ( $\approx 4$  yrs) and are more likely due to surface oscillations. Long-term brightness trends were seen for both stars and appear related with the RVs.

#### 4.15. Stellar Masses of Red Giants from Their Granulation Signal

A sample of 23 RG stars in the range  $1.6 < V < 5.0$  and distributed all over the sky was investigated by Kallinger et al. [116], and a clear granulation and/or oscillation signal was found. Each star was observed almost continuously by at least one of the five BRITE satellites for up to 173 d.

Even though plenty of information is available in the literature for these bright stars, neither surface gravity ( $\log g$ ) nor mass is sufficiently well known. Granulation and/or oscillation timescales, deduced from BRITE-Constellation observations, help to determine model-independent estimates of  $\log g$  with two different methods (Kallinger et al. [117]). Using precise radii from the literature, mostly from interferometric angular diameters and Gaia parallaxes, the mass of the stars can be estimated from  $\log g$ , derived from BRITE-data, which are dominated by the granulation signal.

The stellar masses presented in Figure 22 range from about  $0.7$  to more than  $8 M_{\odot}$  and have formal uncertainties of about 10% to 20%, which covers the observational errors as well as the known uncertainties of the used scaling relations. One might question whether simple scaling relations hold for low-mass giants with about  $10 M_{\odot}$  to high-mass giants with more than  $200 R_{\odot}$ , but this is difficult to estimate due to missing independent and reliable mass estimates. Even though there might still be some unknown systematic effects in the scaling relations, they appear to be at least good enough to disentangle low-mass stars from high-mass stars.



**Figure 22.** Hertzsprung–Russell diagram (left) and Kiel diagram (right) with red giants observed by BRITE-Constellation (grey-filled circles). The small dots show MIST stellar evolution models for solar composition with the mass colour coded. Blue-filled circles mark stars for which solar-type oscillations have been found in the BRITE-Constellation data (adapted Figure 10 from Kallinger et al. [116]).

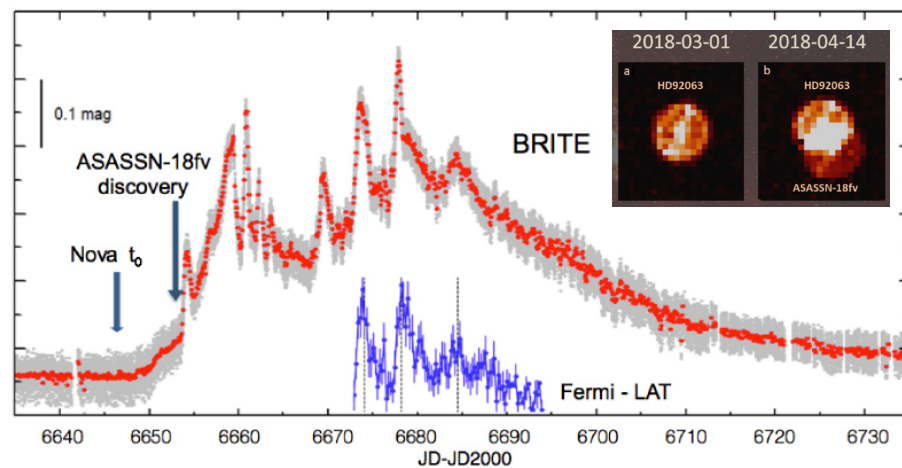
Comparison of the masses derived through the scaling relations with parameters from a large grid of stellar models also allows one to evaluate statistically the relative evolutionary state of the individual stars, that is, to distinguish low-mass red-clump stars from high-mass red giants.

In recent years, the seismology of red giants has grown to become an important field in stellar astrophysics, providing the unique opportunity to probe the interior structure of

evolved stars (Chaplin and Miglio [118]). In general, seismic scaling relations have become indispensable for determining mass and radius of stars with a convective envelope.

#### 4.16. Complete Coverage of Nova Carinae 2018 (ASASSN-18fv)

This first-time ever observation of a *complete* nova eruption came about by chance. The BRITe-Constellation had just monitored 18 stars continuously over several weeks in the constellation Carina, when BRITe-Mission-Control (MC, see Section 3.2) recognised a sudden brightening of a field star (inserts in Figure 23). A quick search among the top sky-news announcements indicated a new star, discovered by the All-Sky Automated Survey for Supernovae (ASASSN) as ASASSN-18fv (Figure 23).



**Figure 23.** BRITe-Toronto photometry of Nova Carinae 2018 (grey: individual observations with red filter, red: orbit averages). Blue: Fermi-LAT (Atwood et al. [119])  $\gamma$ -ray observations. Inserts: raster centred on HD 92063, taken on 1 March 2018 before nova eruption (left), and on 14 April 2018 during nova eruption (right). Scale is  $27''$  per pixel, and exposure times are 4 s.

The cooperation of BRITe-Constellation with the international community is reported, e.g., in Aydi et al. [120] and resulted in unprecedented simultaneous space observations in a broad wavelength range and with BRITe starting even before the actual outburst.

A shock model of Metzger et al. [121] predicts that in addition to  $\gamma$ -rays, the shocked gas should emit mostly in X-rays, which will be absorbed by the dense nova ejecta ahead of the shocked gas, reprocessed to lower energies, and escape in the optical. This process indicates a source for the bolometric luminosity of the nova, in addition to the remnant nuclear burning on the white dwarf surface. Shocks occur in many transient phenomena, such as Type II<sub>n</sub> supernovae, tidal disruption events, stellar mergers, superluminous supernovae, etc. Hence, shock interactions may contribute substantially to the bolometric luminosities of these events, but direct observational evidence has been lacking. The BRITe-Constellation observations were unique in this context and helped to provide insights in many previously poorly observed and understood phases of novae evolution, see for example, Hounsell et al. [122], Aydi et al. [123].

The well-sampled BRITe light curve (Figure 23) clearly resolves a series of distinct short-lasting flares of the order of one to two days, but which were poorly resolved from the ground.  $\gamma$ -rays indicate a series of flares, similar to those in the optical regime, which suggest:

- (i) The fact that the flares occur simultaneously in time in both BRITe bands implies that they very likely share the same origin, that is, shocks, because they power the  $\gamma$ -rays. Consequently, shocks are also powering some of the optical emission.
- (ii) Doubling of the luminosity of the nova during the flares, implies that the shocks power a substantial fraction of the nova luminosity.

- (iii)  $\gamma$ -ray and optical light curves (Figure 23) were very well sampled and indicate a time lag of approximately 5 h. This is an additional confirmation that the optical emission originates in the shocks.  $\gamma$ -rays escape from the shocks with little absorption, but it takes a few hours to reprocess the X-rays and to emit the energy in the optical regime, exactly as observed.

Fortunately, BRITE-Constellation observed this nova even before it was discovered, providing “smoking-gun evidence” for the shock model.

## 5. Summary

BRITE-Constellation has outlasted its minimum design-lifetime by several factors. While it is tempting to terminate the mission, it would be a real pity for humanity to do this, instead of allowing further observations to form a legacy for astronomy. The cost is truly modest compared to most other space missions, especially in relation to the valuable science that BRITE has accomplished and still can accomplish.

BRITE-Constellation’s uniqueness lies first in the small sizes of the individual satellites that are capable of three-axis stabilization and providing a pointing stability accurate enough for astrophysical observations. Second, BRITE-Constellation is an outstanding and unique space mission because of its possibility to observe stars simultaneously in two designated pass-bands and up to 6 months contiguously.

The big success of BRITE-Constellation is reflected—as of March 2021—in 42 peer-reviewed publications and many more conference papers that address a variety of scientific topics from the most massive stars to cool red giants and novae. Here, we have highlighted some of the key results as part of a brief overview.

**Author Contributions:** All authors have contributed substantially to the work reported. All authors have read and agreed to the published version of the manuscript.

**Funding:** We are grateful to BEST, consisting of two voting members per satellite, supplemented by presently 15 non-voting members, who managed BRITE-Constellation successfully during nearly a decade. We acknowledge with thanks the variable star observations from the AAVSO International Database contributed by observers worldwide and used in this research. The authors from Poland acknowledge assistance by BRITE PMN grant 2011/01/M/ST9/05914 and GH thanks the Polish NCN for support (grant 2015/18/A/ST9/00578). AFJM and GAW acknowledge Discovery Grant support from the Natural Sciences and Engineering Research Council (NSERC) of Canada. APo was supported by SUT grant no. 02/140/RGJ21/0012 and Statutory Activities grant no. BK-225/RAu-11/2021.

**Institutional Review Board Statement:** Not applicable.

**Informed Consent Statement:** Not applicable.

**Data Availability Statement:** Data access is provided by <https://brite.camk.edu.pl/pub/index.html>.

**Conflicts of Interest:** The authors declare no conflict of interest.

## References

1. Available online: [http://ntrs.nasa.gov/archive/nasa/casi.ntrs.nasa.gov/19980003950\\_1997125989.pdf](http://ntrs.nasa.gov/archive/nasa/casi.ntrs.nasa.gov/19980003950_1997125989.pdf) (accessed on 1 June 2021).
2. Code, A.; Houck, T.; McNall, J.; Bless, R.; Lillie, C. Ultraviolet Photometry from the Orbiting Astronomical Observatory. I. Instrumentation and Operation. *Astrophys. J.* **1970**, *181*, 97. [CrossRef]
3. Van Duinen, R.; Aalders, J.; Wesselius, P. The ultraviolet experiment onboard the Astronomical Netherlands Satellite-ANS. *Astron. Astrophys.* **1975**, *39*, 159–163.
4. Boggess, A.; Carr, F.; Evans, D. The IUE spacecraft and instrumentation. *Nature* **1978**, *275*, 372–377. [CrossRef]
5. Hall, D. The Space Telescope Observatory. In Proceedings of the Special Session of Commission 44, IAU 18th General Assembly, Patras, Greece, 17–26 August 1982.
6. Van Leeuwen, F.; Evans, D.; Grenon, M.; Grossmann, V.; Mignard, F.; Perryman, M.A.C. The Hipparcos mission: Photometric data. *Astron. Astrophys.* **1997**, *323*, 61–64.
7. Kallinger, T.; Weiss, W. Detecting low amplitude periodicities with Hipparcos. *Astron. Astrophys.* **2002**, *385*, 533–536. [CrossRef]
8. Brown, A. Astrometry and Astrophysics in the Gaia Sky. In Proceedings of the International Astronomical Union, IAU Symposium 330, Nice, France, 24–28 April 2017.

9. Kuschnig, R.; Weiss, W.; Gruber, R.; Bely, P.; Jenkner, H. Microvariability survey with the Hubble Space Telescope Fine Guidance Sensors. Exploring the instrumental properties. *Astron. Astrophys.* **1997**, *328*, 544–550.
10. Kuschnig, R.; Weiss, W.W.; Zwintz, K. Microvariability Survey Based on Photometry with the HST Fine Guidance Sensors. *ASPC* **1998**, *135*, 362.
11. Zwintz, K.; Kuschnig, R.; Weiss, W.W.; Gray, R.O.; Jenkner, H. Hubble Deep Field guide star photometry. *Astron. Astrophys.* **1999**, *343*, 899–903.
12. Weiss, W.W.; Kuschnig, R.; Zwintz, K. Variability Survey with the HST. *ASPC* **2000**, *203*, 38. [[CrossRef](#)]
13. Zwintz, K.; Weiss, W.W.; Kuschnig, R.; Gruber, R.; Frandsen, S.; Gray, R.; Jenkner, H. Variable HST guide stars. *Astron. Astrophys. Suppl. Ser.* **2000**, *145*, 481–490. [[CrossRef](#)]
14. Kuschnig, R.; Weiss, W.; Bahr, R. A Search for Variable Stars based on the HST-FGS Photometry. In Proceedings of the Science with the Hubble Space Telescope- II, Paris, France, 4–8 December 1995.
15. Mangeney, A.; Baglin, A.; Le Contel, J.-M.; Lemaire, P.; Praderie, F.; Vauclair, G. *Projet de Mission Spatiale pour L'étude de la Variabilité et de L'activité des Étoiles: Evris*; CNES: Paris, France, 1982.
16. Vuillemin, A.; Tynok, A.; Baglin, A.; Weiss, W.W.; Auvergne, S.; Repin, S.; Bisnovatyi-Kogan, G. Towards Asteroseismology from Space, the Evris experiment. Optomechanical characteristics and pointing performances of the Evris/PAIS complex. *Exp. Astron.* **1998**, *8*, 257. [[CrossRef](#)]
17. Schneider, J.; Auvergne, M.; Baglin, A.; Michel, E.; Rouan, D.; Appourchoux, T.; Barge, P.; Deleuil, M.; Vuillemin, A.; Catala, C.; et al. The CoRoT Mission: From Structure of Stars to Origin of Planetary Systems. *ASPC* **1998**, *148*, 298.
18. Weiss, W.W.; Baglin, A. High-precision space photometer: CoRoT. In Proceedings of the SPIE, UV, Optical, and IR Space Telescopes and Instruments, Munich, Germany, 29–31 March 2000; Volume 4013, p. 450.
19. Weiss, W.W. Microsatellites. In Proceedings of the Vienna Workshop on the Future of Asteroseismology, Vienna, Austria, 8–12 September 2008; Volume 10, p. 349.
20. Lemaire, P.; Appourchoux, T.; Jones, A.; Catala, C.; Catalano, S.; Frandsen, S.; Weiss, W. PRISMA: A Space Facility for Studying the Rotation; Interior of Stars. *ASP Conf. Ser.* **1992**, *26*, 643.
21. Jones, A.; Gough, D.; Andersen, B.; Baglin, A.; Bisnovatyi-Kogan, G. *SRARS, Seismic Telescope for Astrophysical Research from Space*; ESA: Paris, France, 1996.
22. Favata, F.; Roxburgh, I.; Christensen-Dalsgaard, J. *Eddington A Mission to Map Stellar Evolution through Oscillations and to Find Habitable Planets*; ESA-SCI: Paris, France, 2000; p. 8.
23. Roxburgh, I. Background to the Eddington mission. In Proceedings of the First Eddington Workshop, ESASP, Cordoba, Spain, 11–15 June 2001; Volume 485, p. 11.
24. Plato Science Advisory Team. *Plato: Revealing Habitable Worlds around Solar-Like Stars*; ESA-SCI: Paris, France, 2017.
25. Rucinski, S.; Carroll, K.; Matthews, J.; Stibrany, P. MOST (Microvariability & Oscillation of STars) Canadian Astronomical Micro-Satellite. *AdSpR* **2003**, *31*, 371.
26. Borucki, W.; Koch, D.; Basri, G.; Batalha, N.; Brown, T.; Caldwell, D.; Caldwell, J.; Christensen-Dalsgaard, J.; Cochran, W.; DeVore, E.; et al. Kepler Planet-Detection Mission: Introduction and First Results. *Science* **2010**, *327*, 977–980. [[CrossRef](#)]
27. Hacking, P.; Herter, T.; Stacey, C.; Houck, J.; Shupe, D.; Lonsdale, C.; Gautier, T.N.; Schember, H.R.; Werner, M.W.; Soifer, B.T.; et al. The Wide-Field Infrared Explorer (WIRE) Mission. *ASPC* **1997**, *124*, 432.
28. Eyles, C.; Simnett, G.; Cooke, M.; Jackson, B.; Buffington, A.; Hick, P.P.; Waltham, N.R.; King, J.M.; Anderson, P.A.; Holladay, P.E.; et al. The Solar Mass Ejection Imager (SMEI). *Sol. Phys.* **2003**, *217*, 319–347. [[CrossRef](#)]
29. Ricker, G.; Winn, J.; Vanderspek, R.; Latham, D.; Bakos, G.; Bean, J.; Berta-Thompson, Z.K.; Brown, T.M.; Buchhave, L.; Butler, N.R.; et al. The Transiting Exoplanet Survey Satellite (TESS). *SPIE Proc. Vol.* **2014**, *9143*, 556.
30. Cunha, M.; Antoci, V.; Holdsworth, D.; Kurtz, D.; Balona, L.; Bognar, Z.; Bowman, D.M.; Guo, Z.; Kolaczek-Szymanski, P.A.; Lares-Martiz, M.; et al. Rotation and pulsation in Ap stars: First light results from TESS sectors 1 and 2. *Mon. Not. R. Astron. Soc.* **2019**, *487*, 3523–3549. [[CrossRef](#)]
31. Antoci, V.; Cunha, M.; Bowman, D.; Murphy, S.; Kurtz, D.; Weiss, W. The first view of  $\delta$  Scuti and  $\gamma$  Doradus stars with the TESS mission. *Mon. Not. R. Astron. Soc.* **2019**, *490*, 4040–4059. [[CrossRef](#)]
32. Bowman, D.M. Asteroseismology of high-mass stars: New insights of stellar interiors with space telescopes. *FrASS* **2020**, *7*, 70. [[CrossRef](#)]
33. Burssens, S.; Simón-Díaz, S.; Bowman, D.; Holgado, G.; Michielsen, M.; de Burgos, A.; Castro, N.; Barbá, R.H.; Aerts, C.; et al. Variability of OB stars from TESS southern Sectors 1–13 and high-resolution IACOB and OWN spectroscopy. *Astron. Astrophys.* **2020**, *639*, 81. [[CrossRef](#)]
34. BRITE. Available online: <https://brite-constellation.at> (accessed on 1 June 2021).
35. Zwintz, K.; Kaiser, A. Proceedings of the first BRITE Workshop. In *Communications in Asteroseismology*; Breger: Vienna, Austria, 2008.
36. Weiss, W.; Rucinski, S.; Moffat, A.; Schwarzenberg-Czerny, A.; Koudelka, O.; Grant, C.C.; Zee, R.E.; Kuschnig, R.; Mochnacki, S.; Matthews, J.M.; et al. BRITE-Constellation: Nanosatellites for precision photometry of bright stars. *Publ. Astron. Soc. Pac.* **2014**, *126*, 573–585. [[CrossRef](#)]
37. Deschamps, N.; Grant, C.; Foisy, D.; Zee, R.; Moffat, A.; Weiss, W. BRITE-Constellation. *Acta Astronaut.* **2009**, *65*, 643. [[CrossRef](#)]
38. Koudelka, O.; Unterberger, M.; Romano, P. Nanosatellites-the BRITE and OPS-SAT missions. *e&i Elektrotechnik Und Inf.* **2014**, *131*, 178–187.



39. Pablo, H.; Whittaker, G.; Popowicz, A.; Mochacki, S.; Kuschnig, R.; Grant, C.C.; Moffat, A.F.J.; Rucinski, S.M.; Matthews, J.M.; Schwarzenberg-Czerny, A.; et al. The BRITE-Constellation nanosatellite mission: Testing, commissioning, and operations. *Publ. Astron. Soc. Pac.* **2016**, *128*, 125001. [[CrossRef](#)]
40. Popowicz, A.; Pigulski, A.; Bernacki, K.; Kuschnig, R.; Pablo, H.; Ramiaramanantsoa, T.; Zocoska, E.; Baade, D.; Handler, G.; Moffat, A.F.J.; et al. BRITE-Constellation: Data processing and photometry. *Astron. Astrophys.* **2017**, *605*, A26. [[CrossRef](#)]
41. Popowicz, A. PSF photometry for BRITE nano-satellite mission. *Proc SPIE* **2018**, *10698*, 1069820.
42. Zwintz, K.; Poretti, E. (Eds.) Small satellites-big science, Second BRITE-Constellation Science Conference, Innsbruck. *Proc. Pol. Astron. Soc. (PPAS)* **2016**, *5*, 15.
43. Neiner, C.; Weiss, W.; Baade, D.; Griffin, E.; Lovekin, C.; Moffat, A. Stars and Their Variability. Observed from Space, Celebrating the 5th Anniversary of BRITE-Constellation. 2019. Available online: <https://starsandspace.univie.ac.at/home/proceeding/> (accessed on 1 June 2021).
44. Zwintz, K.; Van Reeth, T.; Tkachenko, A.; Gössl, S.; Pigulski, A. Constraining the near-core rotation of the  $\gamma$  Doradus star 43 Cygni using BRITE-Constellation data. *Astron. Astrophys.* **2017**, *608*, 103. [[CrossRef](#)]
45. Popowicz, A. Analysis of Dark Current in BRITE Nanostellite CCD Sensors. *Sensors* **2018**, *18*, 479. [[CrossRef](#)]
46. Popowicz, A.; Farah, A. Metastable Dark Current in BRITE Nano-Satellite Image Sensor. *Remote Sens.* **2020**, *12*, 3633. [[CrossRef](#)]
47. Bowman, D.; Burssens, S.; Pedersen, M.; Johnston, C.; Aerts, C.; Buyschaert, B.; Michielsen, M.; Tkachenko, A.; Rogers, T.M.; Edelman, P.V.F.; et al. Low-frequency gravity waves in blue supergiants revealed by high-precision space photometry. *Nat. Astron.* **2019**, *3*, 760–765. [[CrossRef](#)]
48. Ramiaramanantsoa, T.; Moffat, A.; Harmon, R.; Ignace, R.; St-Louis, N.; Vanbeveren, D.; Shenar, T.; Pablo, H.; Richardson, N.D.; Howarth, I.D.; et al. BRITE-Constellation high-precision time-dependent photometry of the early-O-type supergiant  $\zeta$  Puppis unveils the photospheric drivers of its small- and large-scale wind structures. *Mon. Not. R. Astron. Soc.* **2018**, *473*, 5532–5569. [[CrossRef](#)]
49. Nichols, J.; Huenemoerder, D.; Naze, Y.; Lauer, J.; Ignace, R.; Miller, N. The zeta Pup Consortium: Correlated X-ray and optical variability in the O-type supergiant  $\zeta$  Pup. *Astrophys. J.* **2021**, *906*, 89. [[CrossRef](#)]
50. Lenoir-Craig, G.; St-Louis, N.; Moffat, A.; Ramiaramanantsoa, T.; Pablo, H. Variability of Wolf-Rayet Stars through MOST(LY) BRITE Eyes. In Proceedings of the Conference Stars and Their Variability Observed from Space, Vienna, Austria, 19–23 August 2019.
51. Chené, A.; St-Louis, N.; Moffat, A.; Schnurr, O.; Crowther, P.; Wade, G.A.; Richardson, N.D.; Baranec, C.; Ziegler, C.A.; Law, N.M.; et al. BinaMiCS Collaboration: Investigating the origin of the spectral line profiles of the Hot Wolf-Rayet Star WR2. *Mon. Not. R. Astron. Soc.* **2019**, *484*, 5834–5844. [[CrossRef](#)]
52. Chené, A.; St-Louis, N.; Moffat, A.; Gayley, K. Clumping in the Winds of Wolf-Rayet Stars. *Astrophys. J.* **2020**, *903*, 113. [[CrossRef](#)]
53. Ramiaramanantsoa, T.; Ignace, R.; Moffat, A.; St-Louis, N.; Shkolnik, E.; Popowicz, A.; Kuschnig, R.; Pigulski, A.; Wade, G.A.; Handler, G.; et al. The chaotic wind of WR 40 as probed by BRITE. *Mon. Not. R. Astron. Soc.* **2019**, *490*, 5921–5930. [[CrossRef](#)]
54. Ramiaramanantsoa, T.; Ratnasingam, R.; Shenar, T.; Moffat, A.; Rogers, T.; Popowicz, A.; Kuschnig, R.; Pigulski, A.; Handler, G.; Wade, G.A.; et al. A BRITE view on the massive O-type supergiant V973 Scorpii: Hints towards internal gravity waves or sub-surface convection zones. *Mon. Not. R. Astron. Soc.* **2018**, *480*, 972–986. [[CrossRef](#)]
55. Richardson, N.; Russell, C.; St-Jean, L.; Moffat, A.; St-Louis, N.; Shenar, T.; Pablo, H.; Hill, G.M.; Ramiaramanantsoa, T.; Corcoran, M.; et al. The variability of the BRITE-est Wolf-Rayet binary,  $\gamma^2$  Velorum-I. Photometric and spectroscopic evidence for colliding winds. *Mon. Not. R. Astron. Soc.* **2017**, *471*, 2715–2729. [[CrossRef](#)]
56. Pablo, H.; Richardson, N.; Fuller, J.; Rowe, J.; Moffat, A.; Kuschnig, R.; Popowicz, A.; Handler, G.; Neiner, C.; Pigulski, A.; et al. The most massive heartbeat: An in-depth analysis of  $\iota$  Orionis. *Mon. Not. R. Astron. Soc.* **2017**, *467*, 2494–2503. [[CrossRef](#)]
57. Shultz, M.; Wade, G.; Alecian, E. BinaMiCS Collaboration: Detection of magnetic fields in both B-type components of the  $\epsilon$  Lupi system: A new constraint on the origin of fossil fields? *Mon. Not. R. Astron. Soc.* **2015**, *454*, L1–L5. [[CrossRef](#)]
58. Pablo, H.; Shultz, M.; Fuller, J.; Wade, G.A.; Paunzen, E.; Mathis, S.; Le Bouquin, J.-B.; Pigulski, A.; Handler, G.; Alecian, E.; et al.  $\epsilon$  Lupi: Measuring the heartbeat of a doubly-magnetic massive binary with BRITE-Constellation. *Mon. Not. R. Astron. Soc.* **2019**, *488*, 64–77.
59. Richardson, N.; Pablo, H.; Sterken, C.; Pigulski, A.; Koenigsberger, C.; Moffat, A.F.J.; Madura, T.I.; Hamaguchi, K.; Corcoran, M.F.; Damineli, A.; et al. BRITE-Constellation reveals evidence for pulsations in the enigmatic binary  $\eta$  Carinae. *Mon. Not. R. Astron. Soc.* **2018**, *475*, 5417–5423. [[CrossRef](#)]
60. Van Genderen, A.; Sterken, C.; de Groot, M.; Stahl, O.; Andersen, J.; Andersen, M.I.; Caldwell, J.A.R.; Casey, B.; Clement, R.; Corradi, W.J.B.; et al. A pulsating star inside  $\eta$  Carinae I. Light variations 1992–1994. *Astron. Astrophys.* **1995**, *304*, 415.
61. Sterken, C.; de Groot, M.; van Genderen, A. A pulsating star inside  $\eta$  Carinae. II. The variability of the pulsation period. *Astron. Astrophys. Suppl. Ser.* **1996**, *116*, 9–14.
62. Goldberg, L. The variability of alpha Orionis. *Publ. Astron. Soc. Pac.* **1984**, *96*, 366. [[CrossRef](#)]
63. Dupree, A.; Baliunas, S.; Guinan, E.; Hartmann, L.; Nassiopoulou, G.; Sonneborn, G. Periodic Photospheric and Chromospheric Modulation in Alpha Orionis (Betelgeuse). *Astrophys. J.* **1987**, *317*, L85–L89. [[CrossRef](#)]
64. Smith, M.; Patten, B.; Goldberg, L. Radial Velocity Variations in Alpha Orionis, Alpha Scorpii, and Alpha Herculis. *Astron. J.* **1989**, *98*, 2233. [[CrossRef](#)]



65. Kiss, L.; Szabó, G.; Bedding, T. Variability in red supergiant stars: Pulsations, long secondary periods and convection noise. *Mon. Not. R. Astron. Soc.* **2006**, *372*, 1721–1734. [[CrossRef](#)]
66. Strassmeier, K.; Granzer, T.; Weber, M.; Woche, M.; Andersen, M.; Bartus, J.; Bauer, S.-M.; Dionies, F.; Popow, E.; Fechner, T.; et al. The STELLA robotic observatory. *Stromische Nachr. Astron. Notes* **2004**, *325*, 527–532. [[CrossRef](#)]
67. Dupree, A.; Strassmeier, K.; Matthews, L.; Uitenbroek, H.; Calderwood, T.; Granzer, T.; Guinan, E.F.; Leike, R.; Montarges, M.; Richards, A.M.S.; et al. Spatially Resolved Ultraviolet Spectroscopy of the Great Dimming of Betelgeuse. *Astrophys. J.* **2020**, *899*, 68. [[CrossRef](#)]
68. Meynet, G.; Haemmerlé, L.; Ekström, S.; Georgy, C.; Groh, J.; Maeder, A. The past and future evolution of a star like Betelgeuse. *EAS Publ. Ser.* **2013**, *60*, 17–28. [[CrossRef](#)]
69. Shultz, M.; Wade, G.; Rivinius, T.; Neiner, C.; Henrichs, H.; Marcolino, W.; MiMeS Collaboration. The pulsating magnetosphere of the extremely slowly rotating magnetic  $\beta$  Cep star  $\zeta^1$  Cma. *Mon. Not. R. Astron. Soc.* **2017**, *471*, 2286–2310. [[CrossRef](#)]
70. Oskinova, L.; Nazé, Y.; Todt, H.; Huenemoerder, D.; Ignace, R.; Hubrig, S.; Hamann, W.-R. Discovery of X-ray pulsations from a massive star. *NatCo* **2014**, *5*, 4024. [[CrossRef](#)] [[PubMed](#)]
71. Pigulski, A. The light-time effect as the cause of period changes in beta Cephei stars. II. Sigma Scorpis. *Astron. Astrophys.* **1992**, *261*, 203–208.
72. Jerzykiewicz, M. Long-term period and amplitude variations in  $\beta$  Cephei stars. *NewAR* **1999**, *43*, 455–460. [[CrossRef](#)]
73. Wade, G.; Pigulski, A.; Begy, S.; Shultz, M.; Handler, G.; Sikora, J.; Neilson, H.; Cugier, H.; Erba, C.; Moffat, A.F.J.; et al. Evolving pulsation of the slowly rotating magnetic  $\beta$  Cep star  $\zeta^1$  Cma. *Mon. Not. R. Astron. Soc.* **2020**, *492*, 2762–2774. [[CrossRef](#)]
74. Pigulski, A.; Cugier, H.; Popowicz, A.; Kuschnig, R.; Moffat, A.; Rucinski, S.M.; Schwarzenberg-Czerny, A.; Weiss, W.W.; Handler, G.; Wade, G.A.; et al. Massive pulsating stars observed by BRITe-Constellation I. The triple system  $\beta$  Centauri (Agena). *Astron. Astrophys.* **2016**, *588*, 55. [[CrossRef](#)]
75. Alecian, E.; Kochukhov, O.; Neiner, C.; Wade, G.; de Batz1, B.; Henrichs, H.; Grunhut, J.H.; Bouret, J.-C.; Briquet, M.; Gagne, M.; et al. First HARPSpol discoveries of magnetic fields in massive stars. *Astron. Astrophys.* **2011**, *536*, 6. [[CrossRef](#)]
76. Handler, G.; Rybicka, M.; Popowicz, A.; Pigulski, A.; Kuschnig, R.; Zocoska, E.; Moffat, A.F.J.; Weiss, W.W.; Grant, C.C.; Pablo, H.; et al. Combining BRITe and ground-based photometry for the  $\beta$  Cephei star  $\nu$  Eri: Impact on photometric pulsation mode identification and detection of several g modes. *Mon. Not. R. Astron. Soc.* **2017**, *464*, 2249–2258. [[CrossRef](#)]
77. Daszyńska-Daszkiewicz, J.; Pamyatnykh, A.; Walczak, P.; Colgan, J.; Fontes, C.; Kilcrease, D. Interpretation of the BRITe oscillation data of the hybrid pulsator  $\nu$  Eridani: A call for the modification of stellar opacities. *Mon. Not. R. Astron. Soc.* **2017**, *466*, 2284–2293. [[CrossRef](#)]
78. Daszyńska-Daszkiewicz, J.; Walczak, P.; Pamyatnykh, A.; The BRITe Team. What Have We Learnt About B-Type Main Sequence Pulsators from the BRITe Data? *PTA Proc.* **2018**, *8*, 65.
79. Walczak, P.; Daszyńska-Daszkiewicz, J.; Pigulski, A.; Pamyatnykh, A.; Moffat, A.; Handler, G.; Pablo, H.; Popowicz, A.; Wade, G.; Weiss, W.W.; et al. Seismic modelling of early B-type pulsators observed by BRITe-I.  $\theta$  Ophiuchi. *Mon. Not. R. Astron. Soc.* **2019**, *485*, 3544–3557. [[CrossRef](#)]
80. Jerzykiewicz, M.; Pigulski, A.; Handler, G.; Moffat, A.; Popowicz, A.; Handler, G.; Pablo, H.; Popowicz, A.; Wade, G.; Weiss, W.W.; et al. BRITe-Constellation photometry of  $\pi^5$  Orionis, an ellipsoidal SPB variable. *Mon. Not. R. Astron. Soc.* **2020**, *496*, 2391–2401. [[CrossRef](#)]
81. Rivinius, T.; Carciofi, A.; Martayan, C. Classical Be stars. Rapidly rotating B stars with viscous Keplerian decretion disks. *Astron. Astrophys. Rev.* **2013**, *21*, 69. [[CrossRef](#)]
82. Wang, L.; Gies, D.R.; Peters, G.J. Detection of Additional Be+sdO Systems from IUE Spectroscopy. *Astrophys. J.* **2018**, *853*, 156. [[CrossRef](#)]
83. Baade, D.; Pigulski, A.; Rivinius, T.; Wang, L.; Martayan, C.; Handler, G.; Panoglou, D.; Carciofi, A.C.; Kuschnig, R.; Mehner, A.; et al. Short-term variability and mass loss in Be stars. IV. Two groups of closely spaced, approximately equidistant frequencies in three decades of space photometry of  $\nu$  Puppis (B7-8 IIIe). *Astron. Astrophys.* **2018**, *620*, A145. [[CrossRef](#)]
84. Neiner, C.; Lee, U.; Mathis, S.; Saio, H.; Lovekin, C.; Augustson, K. Transport of angular momentum by stochastically excited waves as an explanation for the outburst of the rapidly rotating Be star HD 49330. *Astron. Astrophys.* **2020**, *644*, A9. [[CrossRef](#)]
85. Rivinius, T.; Baade, D.; Stefl, S.; Stahl, O.; Wolf, B.; Kaufer, A. Multiperiodic Line-profile Variability and a Tentative Ephemeris for Line-Emission Outbursts of the Be Star  $\mu$  Cen. *ASP Conf. Ser.* **1998**, *135*, 343.
86. Haubois, X.; Carciofi, A.; Rivinius, T.; Okazaki, A.; Bjorkman, J. Dynamical Evolution of Viscous Disks around Be Stars. I. Photometry. *Astrophys. J.* **2012**, *756*, 156. [[CrossRef](#)]
87. Baade, D.; Rivinius, T.; Pigulski, A.; Carciofi, A.; Martayan, C.; Moffat, A.F.J.; Wade, G.A.; Weiss, W.W.; Grunhut, J. Short-term variability and mass loss in Be stars. I. BRITe satellite photometry of  $\eta$  and  $\mu$  Centauri. *Astron. Astrophys.* **2016**, *588*, 56. [[CrossRef](#)]
88. Baade, D.; Pigulski, A.; Rivinius, T.; Carciofi, A.; Panoglou, D.; Ghoreyshi, M.R.; Handler, G.; Kuschnig, R.; Moffat, A.F.J.; Pablo, H.; et al. Short-term variability and mass loss in Be stars. III. BRITe and SMEI satellite photometry of 28 Cygni. *Astron. Astrophys.* **2018**, *610*, A70. [[CrossRef](#)]
89. Baade, D.; Rivinius, T.; Pigulski, A.; Panoglou, D.; Carciofi, A.; Handler, G.; Kuschnig, R.; Martayan, C.; Mehner, A.; Moffat, A.F.J.; et al. BRITening up the Be Phenomenon. 3rd BRITe Science Conference. *Proc. Pol. Acad. Sci.* **2018**, *8*, 69.
90. Stefl, S.; Baade, D.; Rivinius, T.; Stahl, O.; Wolf, B.; Kaufer, A. Circumstellar Quasi-periods Accompanying Stellar Periods of Be Stars. *ASP Conf. Ser.* **1998**, *135*, 348.

91. Labadie-Bartz, J.; Carciofi, A.; de Amorim, T.; Rubio, A.; Luiz, A. Classifying Be star variability with TESS I: The southern ecliptic. *arXiv* **2020**, arXiv:2010.13905.
92. Labadie-Bartz, J.; Baade, D.; Carciofi, A.; Rubio, A.; Rivinius, T.; Borre, C.C.; Martayan, C.; Siverd, R.J. Short-term variability and mass loss in Be stars—VI. Frequency groups in  $\gamma$  Cas detected by TESS. *Mon. Not. R. Astron. Soc.* **2021**, *502*, 242–259. [[CrossRef](#)]
93. Baade, D.; Rivinius, T. The demystification of classical Be stars through space photometry. In Proceedings of the Conference Stars and their Variability Observed from Space, Vienna, Austria, 19–23 August 2019; p. 35.
94. Borre, C.; Baade, D.; Pigulski, A.; Panoglou, D.; Weiss, A.; Rivinius, T.; Handler, G.; Moffat, A.F.J.; Popowicz, A.; Wade, G.A.; et al. Short-term variability and mass loss in Be stars. V. Space photometry and ground-based spectroscopy of  $\gamma$  Cas. *Astron. Astrophys.* **2020**, *635*, 140 [[CrossRef](#)]
95. Smith, M.; Henry, G. Automated photometry of  $\gamma$  Cassiopeiae: The last roundup. *arXiv* **2021**, arXiv:2103.03972.
96. Rucinski, S.M.; Pigulski, A.; Popowicz, A.; Kuschnig, R.; Kozłowski, S.; Moffat, A.F.J.; Pavlovski, K.; Handler, G.; Pablo, H.; Wade, G.A.; et al. Light-curve instabilities of  $\beta$  Lyrae observed by the BRITe satellites. *Astrophys. J.* **2018**, *156*, 12. [[CrossRef](#)]
97. Rucinski, S.; Pigulski, A.; Kuschnig, R.; Moffat, A.; Popowicz, A.; Pablo, H.; Wade, G.A.; Weiss, W.W.; Zwintz, K. Photometry of  $\beta$  Lyrae in 2018 by the BRITe satellites. *Astrophys. J.* **2019**, *158*, 148. [[CrossRef](#)]
98. Kelly, B.; Bechtold, J.; Siemiginowska, A. Are the Variations in Quasar Optical Flux Driven by Thermal Fluctuations? *Astrophys. J.* **2009**, *698*, 895. [[CrossRef](#)]
99. Zu, Y.; Kochanek, C.; Kozłowski, S.; Udalski, A. Is Quasar Optical Variability a Damped Random Walk? *Astrophys. J.* **2013**, *765*, 106. [[CrossRef](#)]
100. Aerts, C.; Mathis, S.; Rogers, T. Angular Momentum Transport in Stellar Interiors. *Annu. Rev. Astron. Astrophys.* **2019**, *57*, 35–78. [[CrossRef](#)]
101. Kallinger, T.; Weiss, W.; Beck, P.; Pigulski, A.; Kuschnig, R.; Tkachenko, A.; Pakhomov, Y.; Ryabchikova, T.; Lüftinger, T.; Palte, P.L.; et al. Triple system HD 201433 with a SPB star component seen by BRITe-Constellation: Pulsation, differential rotation, and angular momentum transfer. *Astron. Astrophys.* **2017**, *603*, 13. [[CrossRef](#)]
102. Paxton, B.; Bildsten, L.; Dotter, A.; Herwig, F.; Lesaffre, P.; Timmes, F. Modules for Experiments in Stellar Astrophysics (MESA). *Astrophys. J. Suppl. Ser.* **2011**, *192*, 3. [[CrossRef](#)]
103. Paxton, B.; Cantiello, M.; Arras, P.; Bildsten, L.; Brown, E.; Dotter, A.; Mankovich, C.; Montgomery, M.H.; Stello, D.; Timmes, F.X.; et al. Modules for Experiments in Stellar Astrophysics (MESA): Planets, Oscillations, Rotation, and Massive Stars. *Astrophys. J. Suppl. Ser.* **2013**, *208*, 4. [[CrossRef](#)]
104. Lous, M.; Weenk, E.; Kenworthy, M.; Zwintz, K.; Kuschnig, R. A search for transiting planets in the  $\beta$  Pictoris system. *Astron. Astrophys.* **2018**, *615*, 145. [[CrossRef](#)]
105. Kenworthy, M.; Mellon, S.; Bailey, J.; Stuik, R.; Dorval, P.; Talens, G.J.J.; Crawford, S.R.; Mamajek, E.E.; Laginja, I.; Ireland, M.; et al. The  $\beta$  Pictoris b Hill sphere transit campaign. Paper I: Photometric limits to dust and rings. *Astron. Astrophys.* **2021**, *648*, 15. [[CrossRef](#)]
106. Zwintz, K.; Reese, D.; Neiner, C.; Pigulski, A.; Kuschnig, R.; Müllner, M.; Zieba, S.; Abe, L.; Guillot, T.; Handler, G.; et al. Revisiting the pulsational characteristics of the exoplanet host star  $\beta$  Pictoris. *Astron. Astrophys.* **2019**, *678*, 28. [[CrossRef](#)]
107. Kurtz, D.; Cropper, M. The Discovery of 6.8 Minute Oscillations in  $\alpha$  Cir. *IBVS* **1981**, *1987*, 1–3.
108. Holdsworth, D.; Brunsten, E. SALT HRS Capabilities for Time Resolved Pulsation Analysis: A Test with the roAp Star  $\alpha$  Circini. *Publ. Astron. Soc. Pac.* **2020**, *132*, 105001. [[CrossRef](#)]
109. Weiss, W.; Froehlich, H.; Pigulski, A.; Popowicz, A.; Huber, D.; Kuschnig, R.; Moffat, A.F.J.; Matthews, J.M.; Saio, H.; Schwarzenberg-Czerny, A.; et al. The roAp star  $\alpha$  Circinus as seen by BRITe-Constellation. *Astron. Astrophys.* **2016**, *588*, 54. [[CrossRef](#)]
110. Weiss, W.W.; Froehlich, H.-E.; Kallinger, T.; Kuschnig, R.; Popowicz, A.; Baade, D.; Buzasi, D.; Handler, G.; Kochukhov, O.; Koudelka, O.; et al. New BRITe-Constellation observations of the roAp star  $\alpha$  Cir. *Astron. Astrophys.* **2020**, *642*, 64. [[CrossRef](#)]
111. Zwintz, K.; Neiner, C.; Kochukhov, O.; Ryabchikova, T.; Pigulski, A.; Müllner, M.; Steindl, T.; Kuschnig, R.; Handler, G.; Moffat, A.F.J.; et al.  $\beta$  Cas: The first  $\delta$  Scuti star with a dynamo magnetic field. *Astron. Astrophys.* **2020**, *643*, 110. [[CrossRef](#)]
112. Lampens, P.; Tkachenko, A.; Lehmann, H.; Deboscher, J.; Aerts, C.; Beck, P.G.; Bloemen, S.; Kochiashvili, N.; Derekas, A.; Smith, J.C.; et al. Low-frequency variations of unknown origin in the Kepler  $\delta$  Scuti star KIC 5988140 = HD 188774. *Astron. Astrophys.* **2013**, *549*, 104. [[CrossRef](#)]
113. Neiner, C.; Wade, G.; Sikora, J. Discovery of a magnetic field in the  $\delta$  Scuti F2m star  $\rho$  Pup. *Mon. Not. R. Astron. Soc.* **2017**, *468*, 46–49. [[CrossRef](#)]
114. Thomson-Paressant, K.; Neiner, C.; Zwintz, K.; Escorza, A. The complex fossil magnetic field of the  $\delta$  Scuti star HD 41641. *Mon. Not. R. Astron. Soc.* **2021**, *500*, 1992–1999. [[CrossRef](#)]
115. Strassmeier, K.; Granzer, T.; Weber, M.; Kuschnig, R.; Pigulski, A.; Popowicz, A.; Moffat, A.F.J.; Wade, G.A.; Zwintz, K.; Handler, G. BRITe photometry and STELLA spectroscopy of bright stars in Auriga: Rotation, pulsation, orbits, and eclipses. *Astron. Astrophys.* **2020**, *644*, 104. [[CrossRef](#)]
116. Kallinger, T.; Beck, P.; Hekker, S.; Huber, D.; Kuschnig, R.; Rockenbauer, M.; Winter, P.M.; Weiss, W.W.; Handler, G.; Moffat, A.F.J.; et al. Stellar masses from granulation and oscillations of 23 bright red giants observed by BRITe-Constellation. *Astron. Astrophys.* **2019**, *624*, 35. [[CrossRef](#)]

117. Kallinger, T.; Hekker, S.; Garcia, R.; Huber, D.; Matthews, J. Precise stellar surface gravities from the time scales of convectively driven brightness variations. *Sci. Adv.* **2016**, *2*, e1500654. [[CrossRef](#)] [[PubMed](#)]
118. Chaplin, W.; Miglio, A. Asteroseismology of Solar-Type and Red-Giant Stars. *Annu. Rev. Astron. Astrophys.* **2013**, *51*, 353. [[CrossRef](#)]
119. Atwood, W.; Abdo, A.; Ackermann, M.; Anderson, B.; Axelsson, M.; Axelsson, M.; Baldini, L.; Ballet, J.; Band, D.L.; Barbiellini, G.; et al. The Large Area Telescope on the Fermi Gamma-ray Space Telescope Mission. *Astrophys. J.* **2009**, *697*, 1071. [[CrossRef](#)]
120. Aydi, E.; Sokolovsky, K.; Chomiuk, L.; Steinberg, E.; Li, K.; Vurm, I.; Metzger, B.D.; Strader, J.; Mukai, K.; Pejcha, O.; et al. Direct evidence for shock-powered optical emission in a nova. *Nat. Astron.* **2020**, *4*, 776–780. [[CrossRef](#)]
121. Metzger, B.; Hascoët, R.; Vurm, I.; Beloborodov, A.; Chomiuk, L.; Sokoloski, J.L.; Nelson, T. Shocks in nova outflows—I. Thermal emission. *Mon. Not. R. Astron. Soc.* **2014**, *442*, 713–731. [[CrossRef](#)]
122. Hounsell, R.; Darnley, M.; Bode, M.; Harman, D.; Surina, F.; Starrfield, S.; Holdsworth, D.L.; Bewsher, D.; Hick, P.P.; Jackson, B.V.; et al. Nova Light Curves From The Solar Mass Ejection Imager (SMEI)—II. The extended catalog. *Astrophys. J.* **2016**, *820*, 104. [[CrossRef](#)]
123. Aydi, E.; Chomiuk, L.; Izzo, L.; Harvey, E.; Leahy-McGregor, J.; Strader, J.; Buckley, D.A.H.; Sokolovsky, K.V.; Kawash, A.; Kochanek, C.S.; et al. Early Spectral Evolution of Classical Novae: Consistent Evidence for Multiple Distinct Outflows. *Astrophys. J.* **2020**, *905*, 62. [[CrossRef](#)]